NOAA Technical Memorandum ERL WMPO-21

U.S. DEPARTMENT OF COMMERCE
NATIONAL OCEANIC AND ATMOSPHERIC ADMINISTRATION
Environmental Research Laboratories

A Case Study of Two Stormfury Cloudline Seeding Events

ROBERT C. SHEETS
SAMUEL C. PEARCE

Weather
Modification
Program Office
BOULDER,
COLORADO
February 1975

NHEML-109

ONMENTAL RESEARCH LABORATORIES

WEATHER MODIFICATION PROGRAM OFFICE

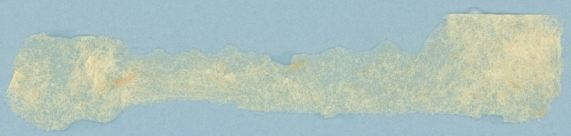

IMPORTANT NOTICE

Technical Memoranda are used to insure prompt dissemination of special studies which, though of interest to the scientific community, may not be ready for formal publication. Since these papers may later be published in a modified form to include more recent information or research results, abstracting, citing, or reproducing this paper in the open literature is not encouraged. Contact the author for additional information on the subject matter discussed in this Memorandum.

NATIONAL OCEANIC AND ATMOSPHERIC ADMINISTRATION

NOAA Technical Memorandum ERL WMPO-21

A CASE STUDY OF TWO STORMFURY CLOUDLINE SEEDING EVENTS

Robert C. Sheets
Samuel C. Pearce

National Hurricane and Experimental Meteorology Laboratory

Weather Modification Program Office
Boulder, Colorado
February 1975

UNITED STATES
DEPARTMENT OF COMMERCE
Frederick B. Dent, Secretary

NATIONAL OCEANIC AND
ATMOSPHERIC ADMINISTRATION
Robert M. White, Administrator

Environmental Research
Laboratories
Wilmot N. Hess, Director

NATIONAL OCEANIC AND ATMOSPHERIC ADMINISTRATION

ENVIRONMENTAL RESEARCH LABORATORIES

National Hurricane and Experimental Meteorology Laboratory

Reports by units of the NOAA Environmental Research Laboratories, contractors, and cooperators working on the hurricane problem are preprinted in this series to facilitate immediate distribution of the information among the workers and other interested units. As the limited reproduction and distribution in this form do not constitute formal scientific publication, reference to a paper in the series should identify it as a preprinted report.

Other reports in this series have been prepared by the National Hurricane Research Project of the U. S. Weather Bureau, by the National Hurricane Research Laboratory, as a part of the Weather Bureau Technical Note Series, and as NHRL Technical Memoranda, a subseries of the Institute of Environmental Research Technical Memoranda series.

Beginning with No. 81, they are identified as NHRL Technical Memoranda, a subseries of the ESSA Research Laboratories (ERL). Beginning with No. 90, they are identified as ERL NHRL Technical Memoranda, a subseries of the NOAA Environmental Research Laboratories (ERL).

Beginning with No. 101, they are identified as ERL WMPO NHRL Technical Memoranda, a subseries of the NOAA Environmental Research Laboratories (ERL), Weather Modification Program Office (WMPO).

Beginning with No. 108, they are identified as ERL WMPO NHEML (National Hurricane and Experimental Meteorology Laboratory) Technical Memoranda.

These reports are available from the National Technical Information Service, Operations Division, Springfield, Virginia 22151 (microfiche: $2.25).

CONTENTS

LIST OF ILLUSTRATIONS

A CASE STUDY OF TWO STORMFURY CLOUDLINE SEEDING EVENTS

Robert C. Sheets and
Samuel C. Pearce

Two cloudline seeding cases were selected for study from the Project STORMFURY cloudline exercises. One case involved clouds in a rather active convective environment while the other case was more isolated. Both cases show that the seeded clouds grew more than surrounding clouds but no unbiased control clouds were monitored. The temperatures at the 550 mb level in the disturbed area were approximately 1C colder than ambient temperatures. This temperature drop is attributed to evaporative cooling in an extremely dry layer which existed at this level. No significant temperature change was noted at the 350 mb level, but at least a temporary increase in the broad scale water vapor content at this level was observed. The duration of these changes is undetermined.

The more isolated and less active cloud group seemed to have little affect on the cloudline scale environment. However, the process of a rapidly developing cloud whose top becomes separated from its base through shearing and entrainment processes is depicted. This process resulted in large localized gradients of moisture and temperature which persisted for some time near the edges of these convective systems.

1. INTRODUCTION

One of the major questions raised by individuals working with numerical models concerns the effects convective systems have upon their environment. This is also a major question addressed by the GATE. We would like to know if and how much these systems warm and/or moisten the environment and at what levels; whether this process makes the environment more stable or conditionally unstable and conducive to future cloud development; why does the system develop or dissipate; is a self-destruction mechanism created, such as a circulation resulting in relatively strong sinking motion in advance of the system which results in entrainment of dry air; what effect does the enhancement of a cloudline have upon neighboring lines. The answers to these questions could have considerable impact upon weather modification and modeling efforts.

Unfortunately, it is difficult to find clear-cut targets of the type for which the STORMFURY experiments were designed and the particular cases studied here were not of the type most desired. Also, the total

energy budget cannot be obtained due to the lack of low-level data and spurious wind fluctuations. However, much can still be learned from such case studies.

Cloudline seeding experiments have been conducted over the past few years as part of the Project STORMFURY field exercises. The primary purpose of these experiments has been to train crews and check out new instruments, seeding agents, and techniques under less demanding conditions than in an actual hurricane modification experiment. In the past, the STORMFURY dry run exercises were conducted prior to or during the cloudline operations in order to acquaint the various U. S. Navy, Air Force, and NOAA crews with the actual seeding and monitoring patterns and operational procedures. Also, individuals are trained to operate various instruments, and each crew determines what equipment is or is not functioning up to the standards required, what requirements are practical or impractical, and what modifications may be necessary in the light of current instrumentation and crew proficiency.

The cloudline operation provides an opportunity for the various crews and scientists to work together collecting data during an actual experiment. In these situations, individuals learn to make decisions concerning in-flight changes necessary to modify pre-existing plans under operational conditions. Making these decisions and recognizing who is responsible for each area, of course, must become spontaneous for the complicated field experiments to be successful. This training cannot be over emphasized; one wrong decision by a senior scientist could jeopardize the entire experiment, or the incorrect operation of a particular instrument could make evaluation of the experiment quite difficult and might possibly jeopardize the safety of the aircraft. The need to be properly prepared becomes even more important when we consider the sparsity of hurricane seeding opportunities under the present rules.

The cloudline and dry run exercises have been quite successful in fulfilling the training requirements stated above. In addition, considerable data have been collected concerning tropical cloud system structure and dynamics. Data collected during a cloudline exercise on August 10, 1971, are the basis for this study directed at developing techniques for analyzing these data; to determine problem areas for use in improving future experiments; as well as determine the cloud characteristics, their response to artificial modification, and their affects upon the surrounding environment.

This particular study is focused on two cloudlines that were seeded and monitored for approximately 1 hour each. The seeder aircraft was a U. S. Air Weather Service WC-130 operating at approximately 19,000 ft. Another AWS WC-130 collected outflow and dropsonde information. A U. S. Navy P3 provided radar coverage and command and control functions. Unfortunately, a receiver malfunction limited the usual dropsonde information and the APS 45 radar system malfunctioned. The NOAA Research Flight Facility (RFF) DC-6 penetrated the clouds at 15,960 ft (550 mb),

while the RFF C-130 performed similar patterns at 26,020 ft (350 mb). The majority of the data analyzed was collected onboard the latter two aircraft.

2. ANALYSIS TECHNIQUES

The temperature, mixing ratio, "D" value, and wind component data recorded at one-second intervals on the two RFF aircraft were analyzed using mathematical filters derived using the variational optimization technique. A detailed discussion of the scheme applied is in Sheets (1973). The response characteristics illustrated in figure 1 are for the filters used in this study. The 1-sec data were averaged over 0.1 n mi intervals for input into the analysis equations. Filter "A" retains nearly the entire signal, filters "C" and "D" retain the response from scales of motion having a wavelength of more than approximately 5 n mi, and 10 n mi, respectively and bandpass filter "E" retains features of .1 n mi to approximately 3 n mi in wavelength. Filters "F" and "G" are centered on 4 to 5 n mi and 10 n mi wavelengths, respectively. That is,

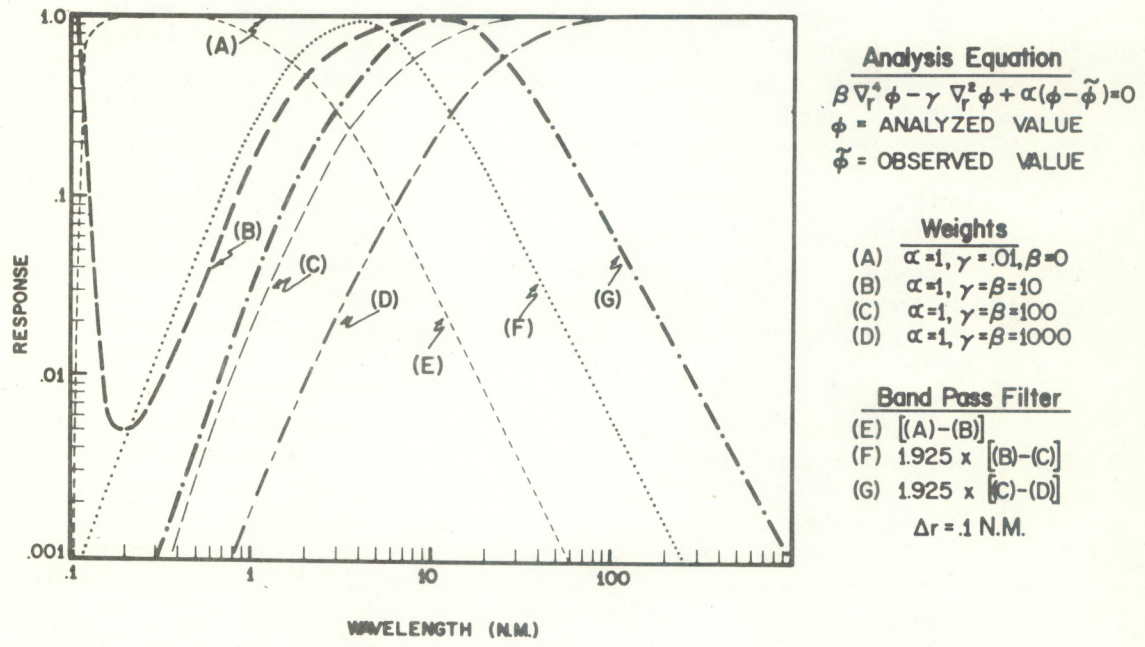

Figure 1. Response curves for low pass and bandpass filters used in analysis.

filter "F" retains nearly 100% of the response generated by scales of motion of 4 to 5 n mi wavelengths, and decreases on either side to less than 20% response at wavelengths of 0.8 and 20 n mi. Likewise, filter "G" effectively retains the response for scales of 3 to 30 n mi in wavelength.

Use of the filters described above permits us to effectively separate the contribution from the various significant scales of motion. If we sample the seeded cloud in a nearly continuous fashion, then seeding response times and characteristics can be determined for the various scales of motion. Also, if adequate data are available this technique enables us to remove the smaller scale components and observe the larger scale changes associated with the cloud system environment. This capability proves quite useful in the analyses. However, the recorded data were insufficient to totally resolve the response characteristics of the smaller scale features, but future experiments can be designed to take advantage of these analytical capabilities.

The RHI radar composites presented later were obtained by the RDR 3.2 cm radar system whose antenna is located in the tail of the RFF DC-6 aircraft. The antenna scans 360 degrees in the vertical plane normal to the aircraft fuselage. This configuration allows us to obtain a vertical cross section of convective elements located within 15 to 20 n mi on either side of the aircraft. This "slicing" process, illustrated in figure 2, shows the RHI presentation as a sequence of "slices" through the cloud as depicted on the RDR radar scope, and an artist's conception of the cloud. The heavy solid-and-dashed arrow in the PPI and cloud presentation indicates the aircraft track relative to the cloud. The small dashed numbered lines show the locations of the vertical slices through the cloud corresponding to the RDR sequence. The appearance of shearing clouds on the RDR scope operated in the contour mode is well illustrated by this case. The effective range varies depending upon how many and how intense the cloud elements are between the short-wavelength low-powered radar and the potential targets. Thus, the short wavelength permits us to observe the weaker cells with small particles, including the anvils or shearing tops, but the signal suffers considerably from attenuation.

The RHI radar composites were obtained by projecting photographs of the radar scope for each scan (7 sec per scan) onto the surface of an x, y digitizer. The echo dimensions were then digitized and recorded on magnetic tape. The cloud height values were machine plotted relative to the aircraft position and heading at intervals 0.25 n mi and were analyzed by hand. The clouds were then contoured (topographic) at intervals of 1,000 feet where 0 represented the radar edge of the cloud. Maximum echo tops were designated by point values. The aircraft track was superimposed (dotted line) and represents the position of the RFF DC-6 aircraft relative to the echoes contained in the illustrations.

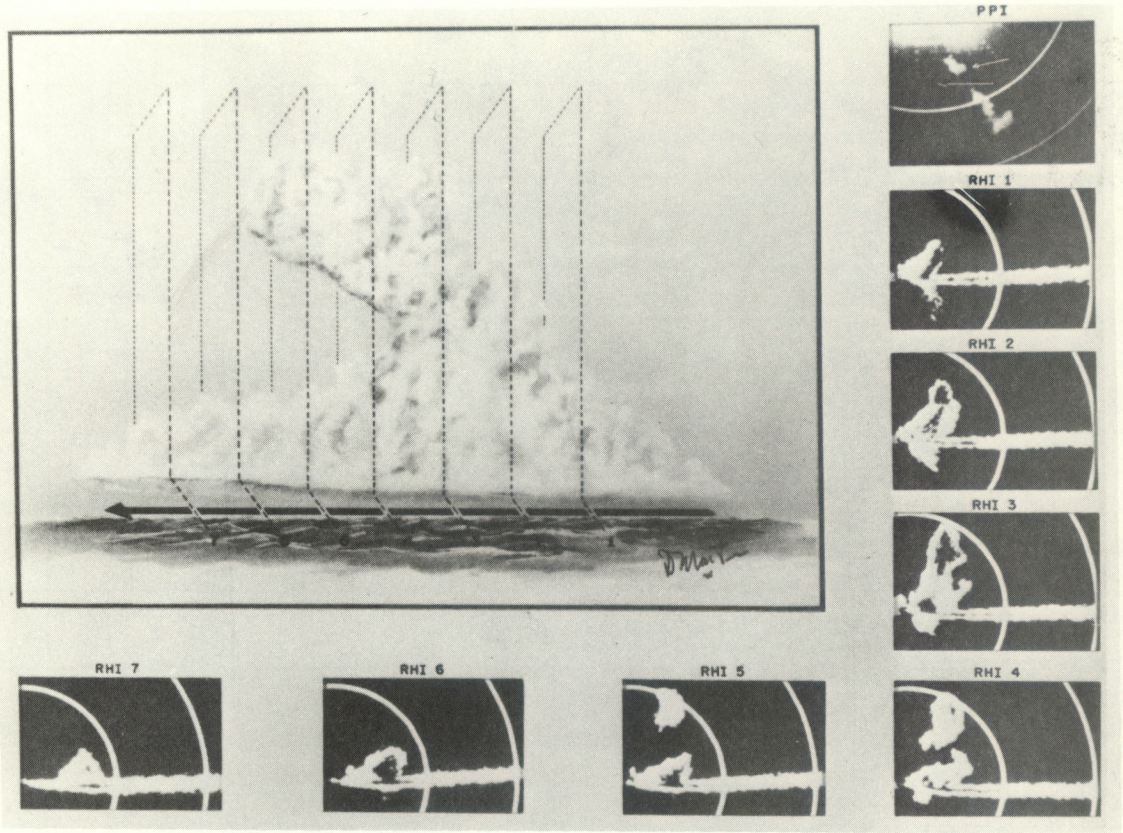

Figure 2. RHI radar depiction of a shearing cloud at 7 sec intervals. The PPI presentation (20 n mi range markers) is shown in the upper right panel. The dark and white arrows are the aircraft track and the cloud being probed, respectively. The RHI presentations (operated in the contour mode with 5 n mi range markers) correspond to the numbered vertical slids through the cloud. The bold dashed arrow is the aircraft track.

3. SYNOPTIC STRUCTURE

The cloudline seeding area for August 10, 1971, was located near 11.5°N and 58°W. The surface analysis performed by the National Hurricane Center (not illustrated) showed the Bermuda-Azores high dominating the large-scale tropospheric circulation in the North Atlantic with ENE surface winds of 15 to 20 kt prevailing in the operational area. The low-level wind analysis (fig. 3) showed the area of concern to be located on the northern edge of the ITCZ. This condition is further substantiated by the superimposed nephanalysis derived from satellite observations. A band of clouds approximately 2° to 3° wide and extending from approximately 35°W to 65°W with a southern boundary located near 10°N is shown. The disturbances on the Inter-Tropical Convergence Zone (ITCZ) located nearest

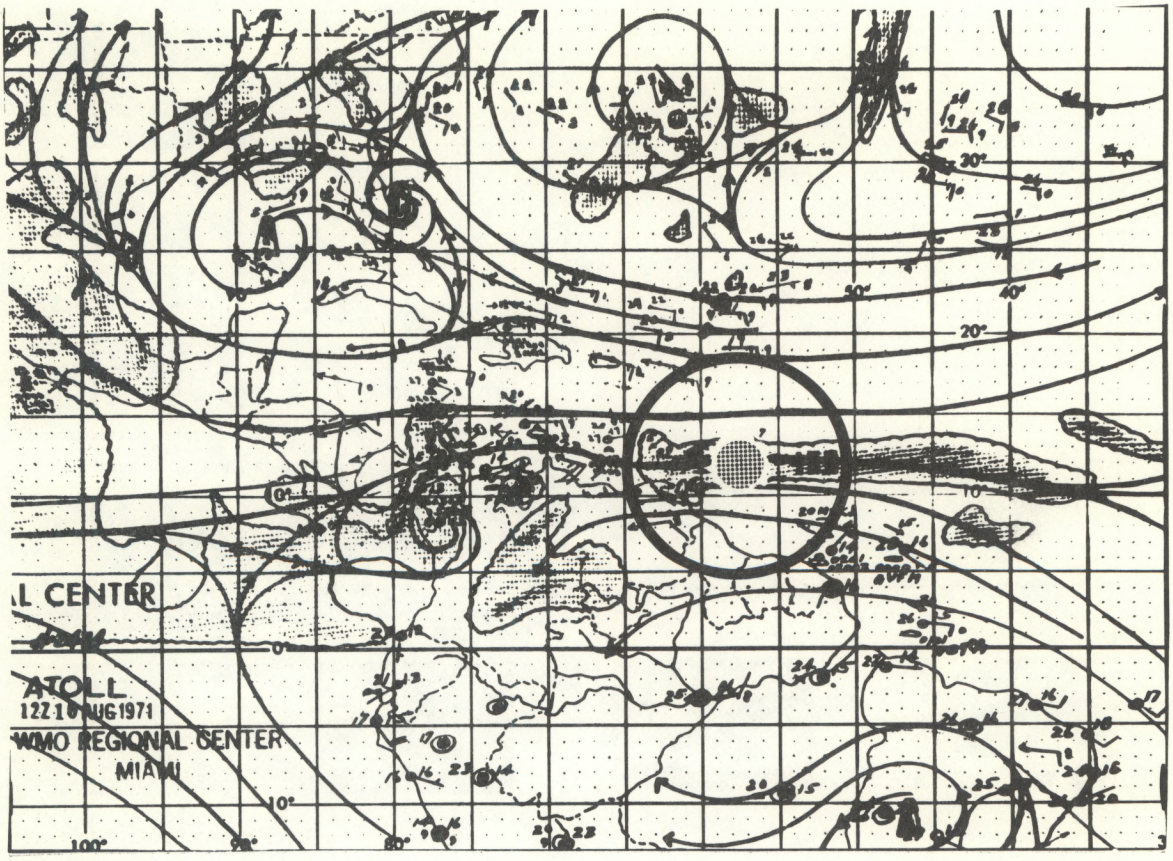

Figure 3. ATOLL analysis for 1200Z August 10, 1971, with superimposed satellite observed cloud cover. The small stipled area inside the large circle was the area of the cloudline operations.

the operational area were near Panama and the western coast of Africa. Ship observations and aircraft data, discussed in detail later, indicated cumulus clouds in the seeding area with tops generally near 20,000 ft and with a few cells extending into a cirrus layer.

The 200 mb analysis (not illustrated) showed a ridge dominating the operational area. The lower troposphere mean circulation (1000 to 600 mb layer) indicated easterly flow of 25 kt while the upper troposphere mean circulation (600 to 200 mb layer) was easterly flow of nearby 20 kt over the area, resulting in a shear between the upper and lower layers of approximately 5 kt. This relatively uniform horizontal flow in the vertical is of course conducive to vertical cloud development. However, the ridge to the north where some upper and middle-level subsidence was occurring suppressed development. This condition was reflected by the radiosonde for Barbados at 1200Z on August 10, 1971. Dewpoint depressions were generally greater than 20C and 750 mb through 300 mb. On the other hand, the lowest 50 mb layer was conditionally unstable with the neutral point being near 950 mb.

The Simpson-Wiggert cumulus cloud model (Simpson and Wiggert, 1969) was run using the Barbados upper air sounding for 1200Z August 10, 1971. The results indicated that we could not get cloud development to a potential seeding level (-4C) until the cloud bubble radius[1] became quite large (1 n mi). Even then, the height of clouds which were initially 25,000 ft would only grow an additional 1,000 ft as a result of the seeding. Only excessive radii would give large cloud growth.

4. CLOUD GROUP I STRUCTURE (1725 to 1840 Z)

It is difficult to catagorize these cloud systems as single cloud lines in the classical sense. As previously mentioned, these systems were SSE of Barbados and were associated with the northern edge of the ITCZ forced convection, embedded in deep easterly flow. The lower tropospheric winds were easterly at about 25 kt while the upper level winds were from nearly the same direction at 20 kt. This particular system was selected because of the absence of more classical systems to the north.

4.1 Radar

Figure 4 shows composites of the PPI radar structure for the first cloud group selected. These composites represent the WP-101 5.6 cm radar system scope presentations during the period listed at the bottom of each panel of figure 4. The tracks for flights 710810B (DC-6) and 710810F (C-130) are superimposed. The relative position of the aircraft to particular cloud elements is only approximate since the clouds were forming, dissipating, and moving through the area.

This rather disorganized system increased considerably in area during the 1-hour monitoring period. The letters indicate corresponding echoes between the two periods. The cloud indicated by A and the cloud immediately to the south were the targets for the seeding, which occurred at approximately 1733Z. Five pyrotechnics were fired on a single pass through this cloud system. The visual cloud merged into a single system even before the seeding. Capt. Davis on the seeder aircraft reported ~ 3.5 m/sec updrafts and moderate rain during the seeding run conducted at an altitude of 19,000 ft and temperature of -9C.

Figure 5 shows the RHI radar composites obtained in the manner described in the Introduction. Flight 710810B penetrated the prospective seeding targets (cloud designated by A) at approximately 1726Z (figs. 4A

---

[1] The radii referred to in the Simpson-Wiggert model is that of the rising bubble, not the entire cloud.

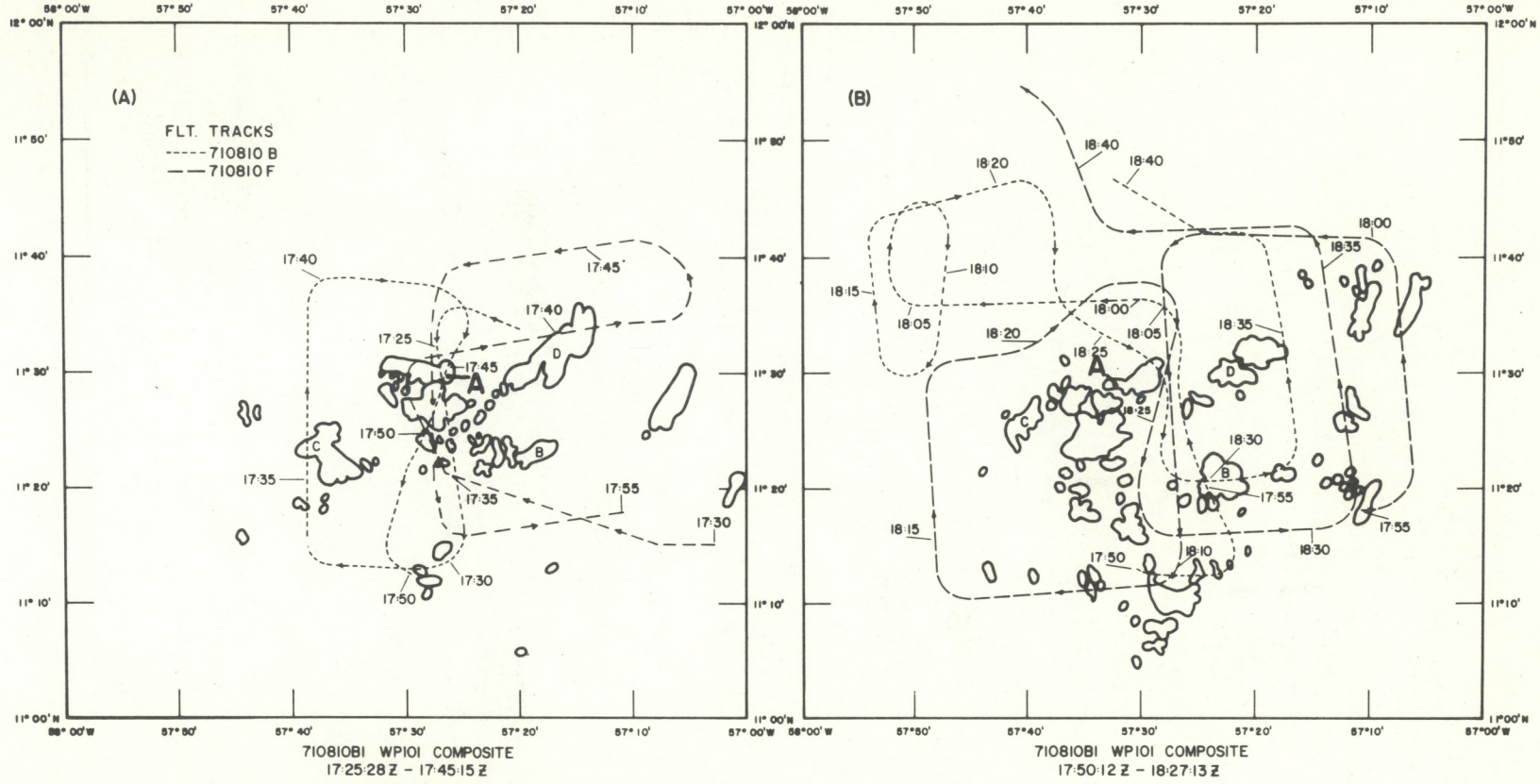

Figure 4. PPI radar composites for cloud group I and superimposed aircraft tracks.

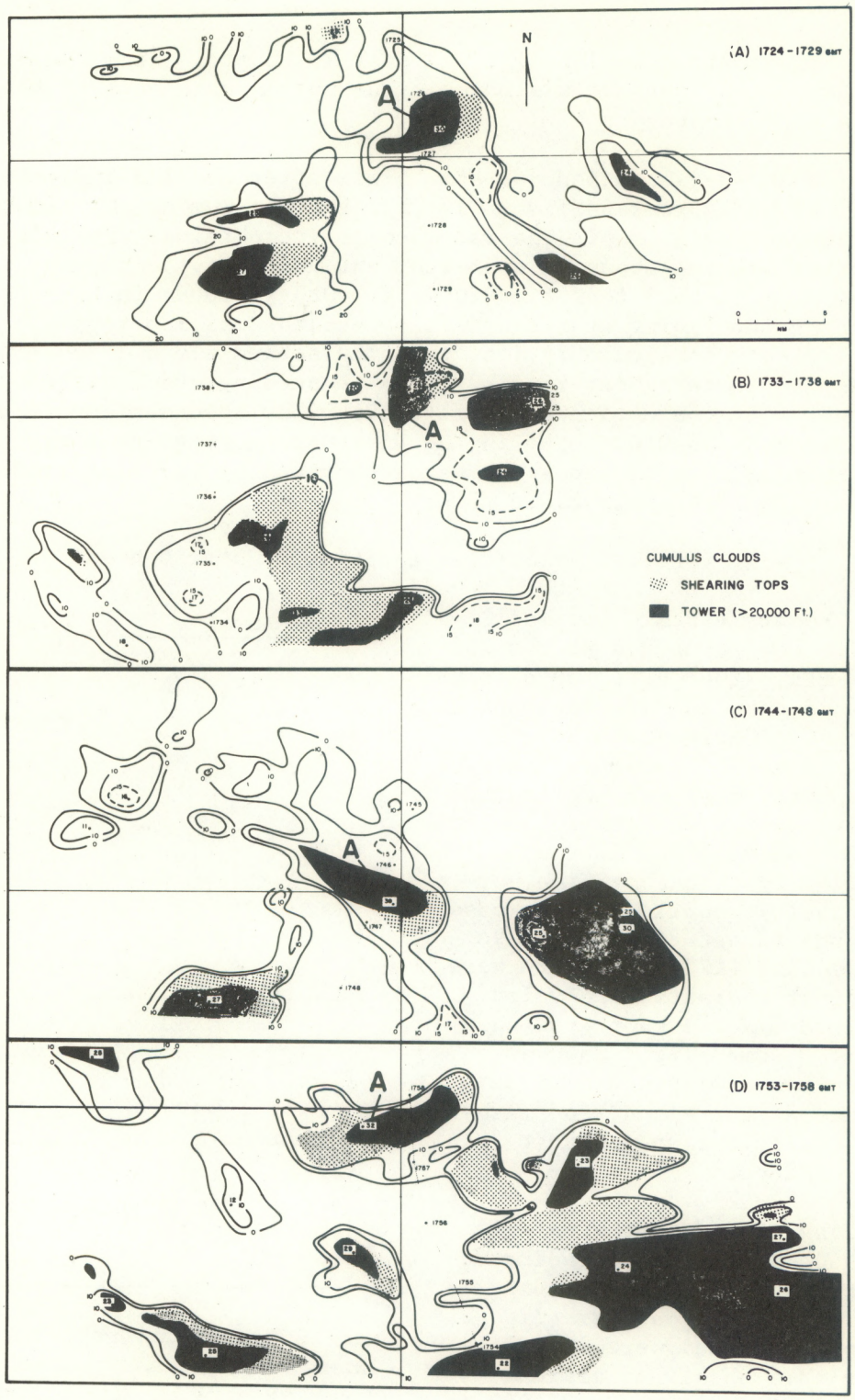

Figure 5. RHI radar composites for cloud group I and superimposed aircraft tracks.

and 5A). The maximum cell height was near 30,000 ft. Some shearing of cloud tops toward the east was noted. The north-south axis of the main cloud was approximately 8 n mi long.

The RHI presentation for some 5 min after seeding indicated the target cloud had spread horizontally, but the maximum height remained nearly the same (fig. 5B). The radar composite obtained approximately 13 min after seeding shows an east-west extension of the core of the cloud and maximum cell tops of 39,000 ft. Other clouds in the area seemed to be developing at the same time but the maximum tops of these radar cells were considerably less than the seeded cloud. The final RHI composite, indicates about 25 min after the seeding event rather massive development over the entire area (fig. 4B). The seeded cloud remained quite large but appeared to be in the dissipating stage as the maximum top was near 32,000 ft, and shearing or overhanging tops occurred both east and west of the main cloud tower.

4.2 Vertical Velocities and Liquid Water Content

The draft scale vertical velocities were computed at the 550 mb level (FLT 710810B) using a technique based upon the displacement of the aircraft (Carlson and Sheets, 1971). The liquid water contents were computed using data collected by a continuous hydrometeor sampler (foil) (Hindman, 1970) at the 550 mb level. Figure 6 shows the vertical velocity profile for the pass through the target cloud (fig. 5A) before seeding (1726Z). There were two distinct updrafts with velocities near 8 m/sec encountered on this pass. Some slight downward motion occurred within 4 n mi on both sides of the cloud, and rather neutral conditions appeared at greater distances.

The liquid water contents at the 550 mb level also indicated two distinct cells corresponding to the updrafts noted earlier (fig. 6). The computed values were near 0.8 gm/m^3 on this pass when maximum radar echo tops were near 30,000 ft. This value is quite low since the

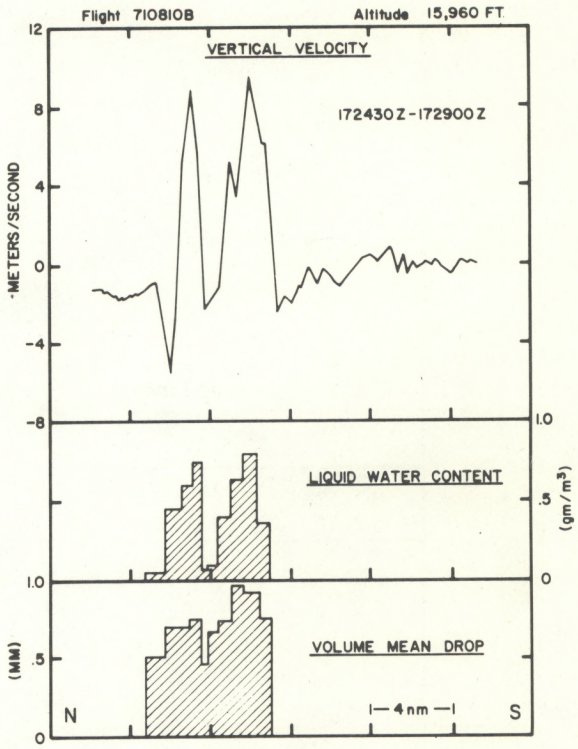

Figure 6. Vertical velocities, liquid water content, and volume mean drop diameter size at the 550 mb level recorded on a pass through the target cloud, before seeding.

adiabatic liquid water content would be near 6 gm/m^3 at this level. These values reflect entrainment of very dry air that existed above the 800 mb level. The volume mean drop diameter size (one half of water by volume contained in larger sized drops and one half in smaller sized drops) variation through the cloud showed the larger size particles were present in the fresh updraft on the south edge of the cloud. Even here, the liquid water contents were relatively low when averaged over the 0.5 n mi interval necessary for obtaining a statistically significant sample. Obviously, higher values would be present in the smaller active bubbles where depletion by entrainment processes would be less.

Figure 7 shows the vertical velocity profiles recorded on two later passes through the seeded cloud. The maximum updrafts some 13 to 15 min after seeding were less intense than previously recorded, but updrafts covered a relatively large area (solid line). This feature corresponds to the larger horizontal extent of the radar echo (figs. 5C and 5D). The vertical velocities between clouds indicated a very small mean upward motion in the areas traversed from 1736 to 1738Z and 174730 to 174830Z and showed neutral conditions from 1727 to 1729Z and 1755 to 1756Z at the 550 mb level. The locations of these measurements relative to the radar presentations may be determined from figure 5. The liquid water content measurements also reflected the less vigorous but greater horizontal extent of the activity at this level (fig. 7) with values generally being between 0.2 and 0.3 gm/m^3. At the same time, the drop size distribution became more uniform with the volume mean drop diameter being near 0.5 mm across the cloud. Unfortunately, these were the last liquid water content measurements made on this flight.

The vertical velocity profile recorded on the last pass through this system (1755Z) at the 550 mb level (dashed line, fig. 7) indicated updrafts generally less than 2 m/sec. However, one cell on the south side of the system had an updraft of near 6 m/sec.

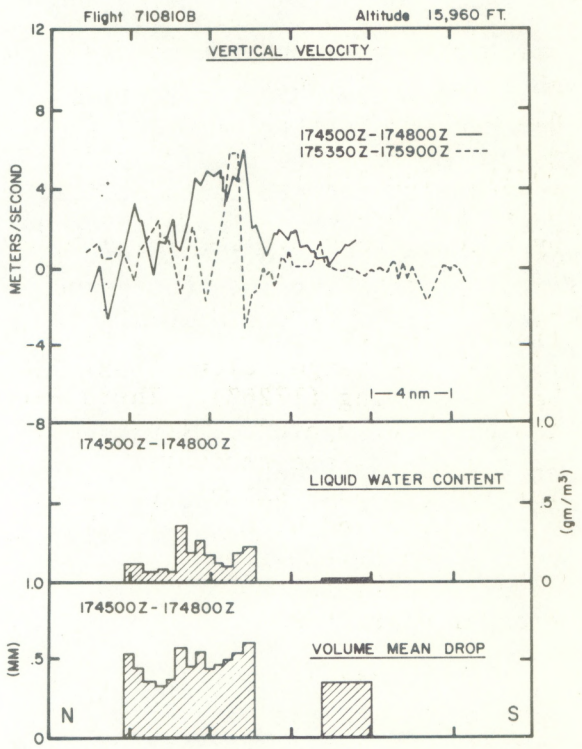

Figure 7. Vertical velocities, liquid water content, and volume mean drop diameter size recorded on two passes through the seeded cloud at the 550 mb level.

4.3 Equivalent Potential Temperature

Figure 8 shows the equivalent potential temperature profiles obtained on the three passes through the target cloud at the 550 mb level. The highest values were obtained on the first pass, which was before the seeding. The maximum value (343A) exceeded ambient values by as much as 18C. The later profiles indicated continued large gradients on the north edge of the system, but general increases in values were recorded south of the main activity. This feature corresponds to the observed increase in convective activity to the south, as shown in the radar composites (figs. 4 and 5).

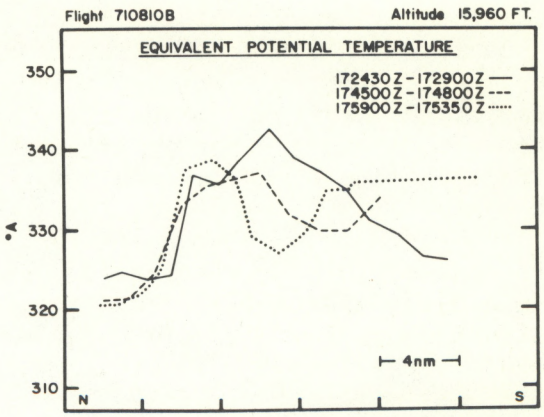

Figure 8. Equivalent potential temperature profiles recorded at the 550 mb level through cloud group I.

The equivalent potential temperature profiles recorded at the 350 mb level (fig. 9) show no large horizontal gradients at this level, since cirrus clouds covered most of the area and the moisture factor was considerably decreased. However, probably the most significant feature in this set of profiles is the general increase that took place over the nearly 40-min monitoring period over almost the entire area covered. This feature was probably a direct result of the increased convective activity discussed earlier (figs. 4 and 5).

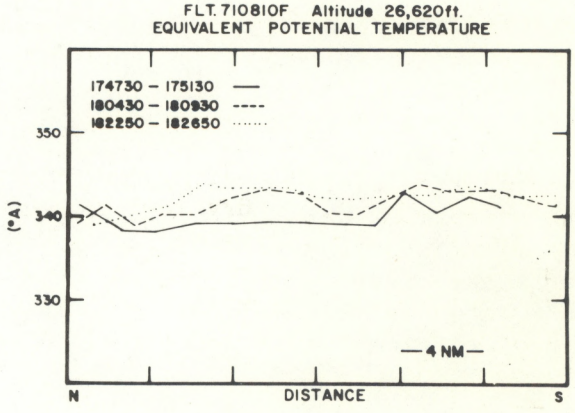

Figure 9. Equivalent potential temperature profiles recorded at the 350 mb level through cloud group I.

4.4 Temperature, Water Vapor, Pressure, and Wind

The filtering scheme described in the introduction was applied to the conventional data collected on north-south passes through the seeded cloud area. The northern half (left side) of the profiles correspond to the immediate area of the seeded cloud (see figs. 4 and 5).

Figure 10 shows the time sequence of profiles recorded at the 550 mb level. The warmest temperature recorded at this level was observed before seeding (solid line) on the southern edge of the target cloud. This region also contained a major updraft as was noted earlier. In fact, the two temperature peaks (filter "A") in the seeding area (left half of profiles) are in the same location as the two peaks shown in the vertical velocity profiles (fig. 6). These apparently were the areas that were seeded some 5 to 6 min later. The vertical velocity became small just outside the south edge of the radar echo (fig. 5) and the temperature decreased by about 4C. This area later warmed while the maximum temperatures located north and south decreased. This feature is quite evident in the profiles for filters "C" and "D". The profiles obtained by application of filter "D" represent the response from scales of motion greater than about 10 n mi in wavelength. The time sequence of profiles (fig. 10) indicates that local warming occurred as discussed above, but the average temperature over the pass remained relatively steady at -3.5C to -4C. The intermediate pass profiles are the smoothest and probably represent the detrainment stage. The first profile (solid line) appears to represent the most active period of the cloud's life cycle, and the last may indicate the beginning of a recycling process.

The mixing ratio profiles indicated nearly saturated conditions throughout the target cloud area (left half of profiles) and then dry conditions on the south side of the cloud (50 percent relative humidities) before seeding. This dry region (center of profile for filter "A") corresponds to the cold region noted in the temperature field. This dry area became more moist later in a change similar to the warming discussed earlier. Note also that even though this area was warming and becoming more moist, a relative cold and dry area remained south of the cloud on all but the last pass through the system. That is, this feature remained prominent for at least 30 min. The last pass through the area, some 30 min later, indicated the nearly complete disappearance of this feature. Another significant feature present in the mixing ratio profiles was the maintenance of a very large moisture gradient on the northern edge of the system. This area probably corresponded to the northern edge of the ITCZ convective activity. Note that the large-scale moisture level, as indicated by the mixing ratio profiles (filter "D") shows little change with time at this level when averaged over the cloud area.

The profiles of "D" values showed large horizontal fluctuations on each pass during the monitoring period (fig. 10). The shaded area is essentially common for the time sequence of profiles exhibited. The

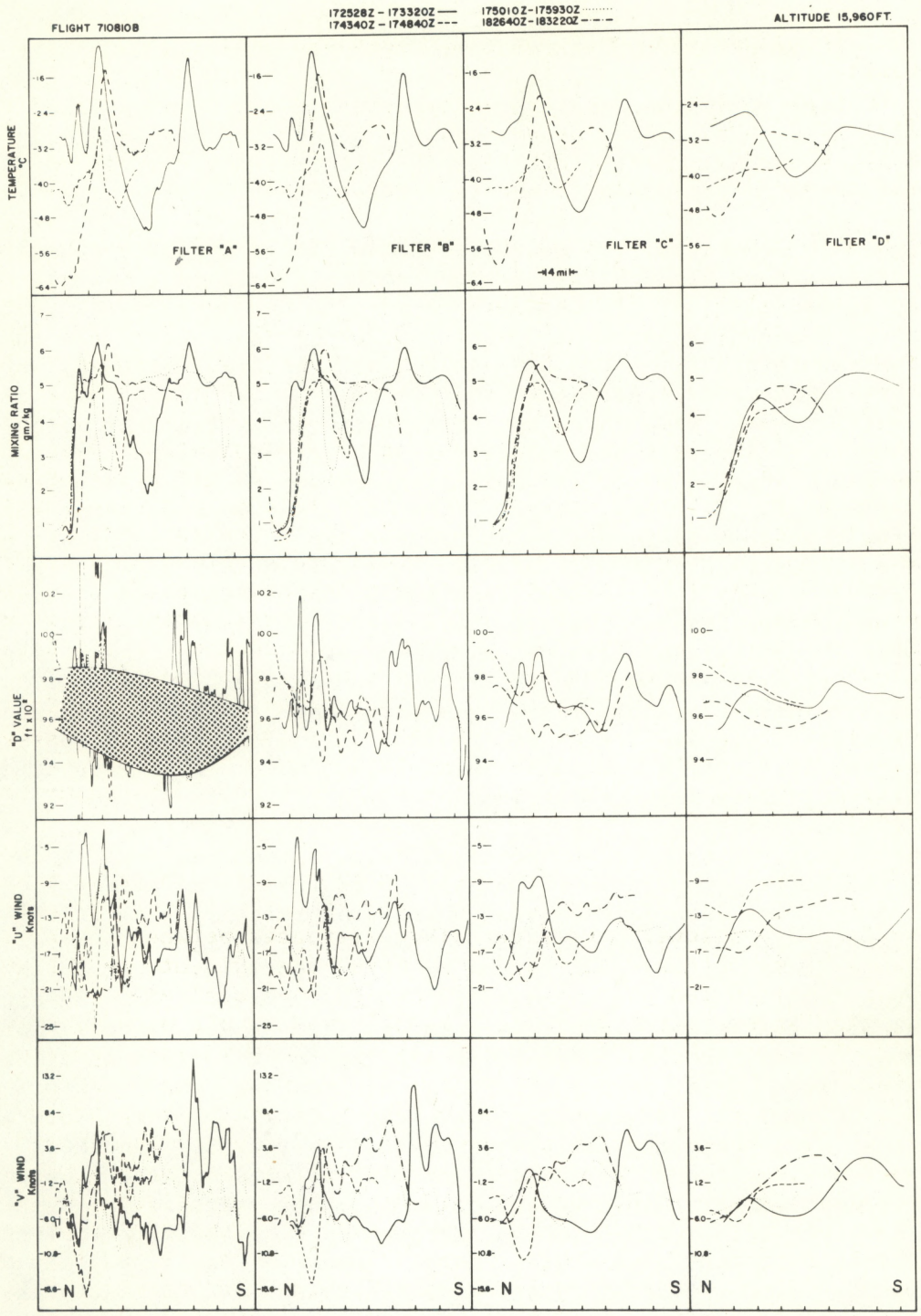

Figure 10. Filtered temperature, mixing ratio, "D" value, and u and v wind component profiles for north-south passes through the seeded cloud area at the 550 mb level.

largest fluctuations were recorded before seeding (solid line, filter "A") where changes of as much as 100 ft were noted over distances of less than 4 n mi. Most of these fluctuations were contained in the shorter wavelength features. These profiles become smoother on the intermediate passes (filters "B" and "C"). The large-scale feature (filter "D") again showed little net change when averaged over the length of the pass.

Large horizontal fluctuations occur in the u and v wind components recorded during the monitoring period. Changes of as much as 15 kt over horizontal distances of less than 4 n mi in both the u and v components were recorded (fig. 10, filter "A"). However, if the contributions from the small-scale features are removed, mean u and v components of about -15 kt and -3 kt result (filter "D").

Figure 11 shows the band filtered temperature, mixing ratio and "D" value profiles for the 550 mb level. This type of presentation allows us to determine the relative magnitudes of significant scales of motion. There is some overlap (see fig. 1) but basically "E" corresponds to bubble scale (0.1 to 3 n mi wavelengths), "F" to cell-scale motion (5 n mi wavelengths), and "G" to cloud scale motion (10 n mi wavelengths). The temperature and mixing ratio profiles indicate that the contribution from approximate bubble-scale motion was generally less than one-half that from cell-scale motion and nearly an order of magnitude less than for the cloud-scale motion. The first and last profiles recorded for these parameters seemed to be the most active, as noted earlier. This feature is amply demonstrated in the cloud-scale motion profiles (filter "G"). The "D" value profiles, however, indicate nearly an equal response for all the scales represented.

Figure 12 shows the temperature, mixing ratio and u and v wind components ("D" values were missing due to equipment malfunction) profiles for the 350 mb level. Considerable differences between these profiles and those obtained at the 550 mb level are evident. The horizontal variations in temperature were generally much smaller at the 350 mb level, the largest variations recorded occurred 30 min after seeding rather than before, and the great percentage of these variations were contained in the shorter wavelength features. No measurements were obtained at this level before seeding, but the temperatures recorded 15 min after seeding showed variations over the cloud area to be generally less than 0.5C as compared to 3C for a similar period at the 550 mb level. The uniformity of temperature is quite evident in the profiles obtained with filter "D" (fig. 12). The mean temperature of about -23C represents a slightly less than moist adiabatic lapse rate from the temperature recorded at the 550 mb level and correlates well with the large scale structure, as discussed earlier, and the 1200Z Barbados sounding for this date.

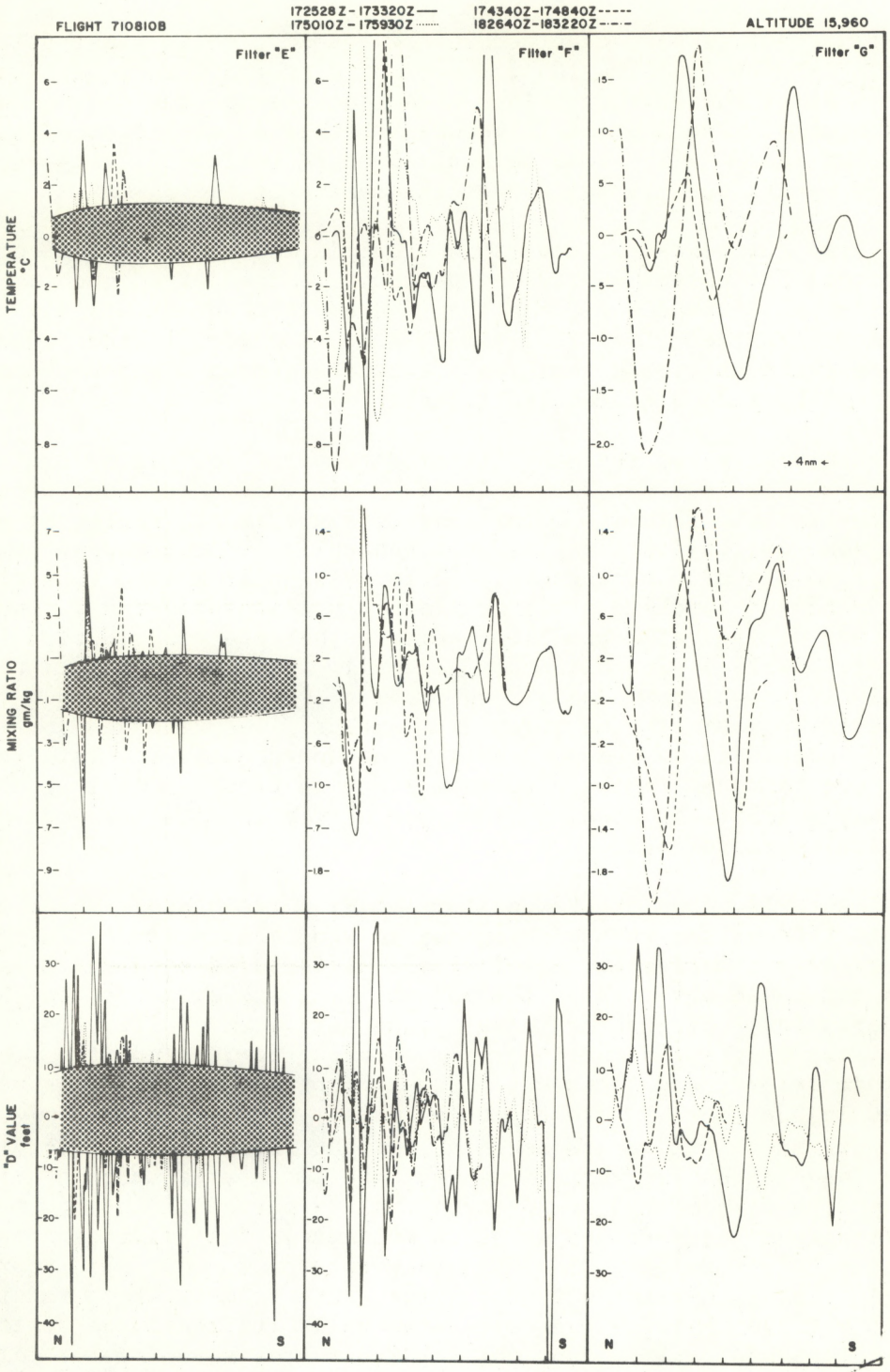

Figure 11. Band filtered temperature, mixing ratio, and "D" value profiles for north-south passes through the seeded cloud area at the 550 mb level.

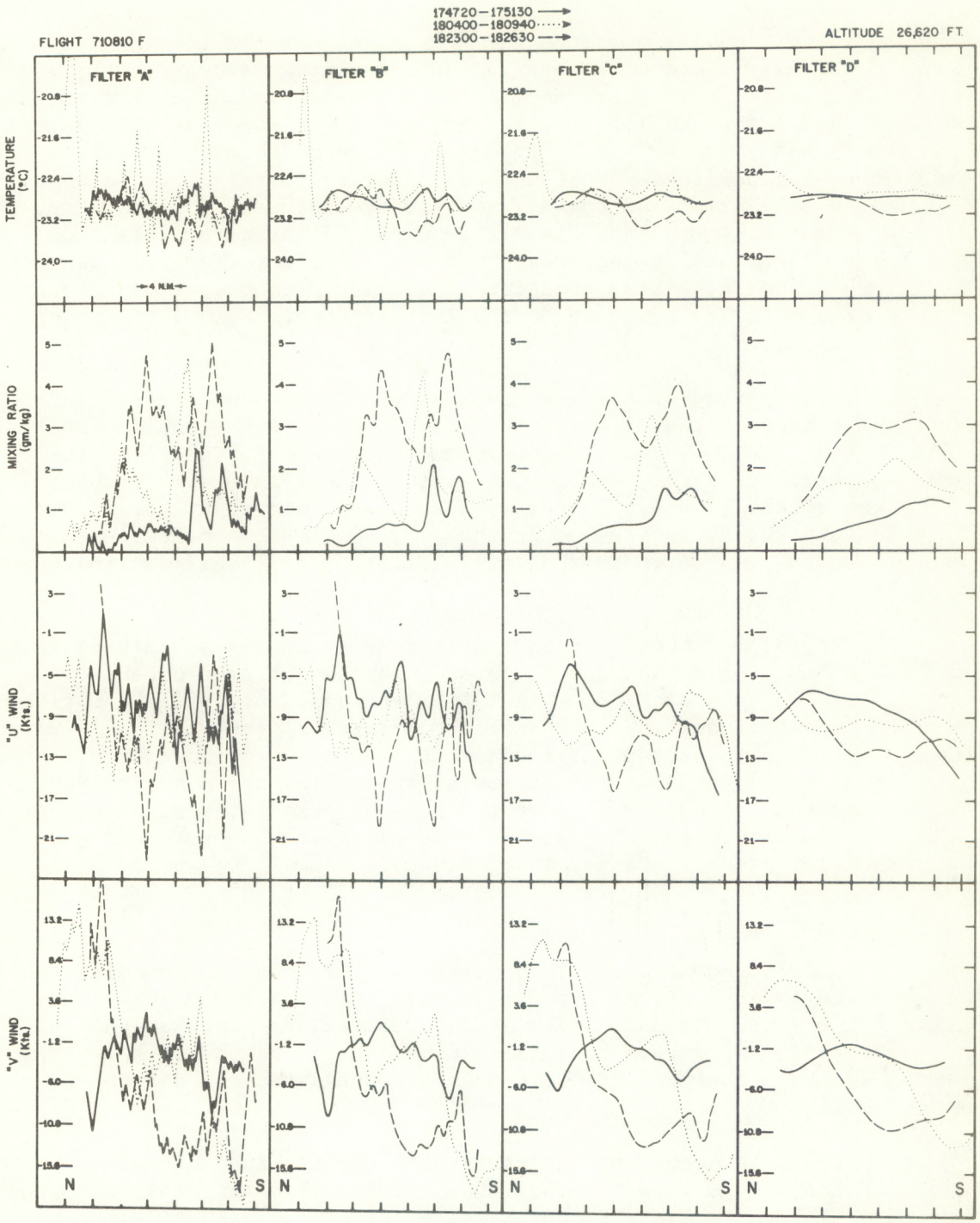

Figure 12. Filtered temperature, mixing ratio, and u and v wind component profiles for north-south passes through the seeded cloud area at the 350 mb level. (Filters same as for fig. 10.)

The mixing ratio values for this level must be interpreted with caution. These values were obtained with an infrared hygrometer, and small calibration errors are amplified in the cold, low water vapor content regions. The absolute values indicate large supersaturations, but the trends and relative values appear to be reasonable. Therefore, we decided to include these important measurements, but ignore the absolute values and concentrate on trends and relative values. For instance, note the large moisture gradient associated with the northern (left) edge of the target cloud region that was present at this level as well as the 550 mb level. Also, a general increase with time in the water vapor content was recorded; values observed on the last pass were 3 to 4 times those recorded on the first pass through this area.

The magnitudes of the horizontal wind component fluctuations were nearly the same at the 350 mb level (fig. 12) as at the 550 mb level (fig. 10). Again, a majority of these fluctuations were contained in the smaller scale features. However, note that the mean easterly component ("D") was generally about 5 kt less than that observed at the lower level. This feature was also observed in the large-scale flow patterns discussed earlier and is reflected in the general tilting of cloud tops toward the east (fig. 5).

Figure 13 shows the band filtered temperatures and mixing ratios for the cloud area at the 350 mb level. The target area became quite active for the bubble ("E"), cell ("F"), and cloud scale ("G") motions some 30 min after seeding. The maximum effects on the recorded mixing ratios, however, occurred in the last pass, which was about 50 min after seeding. The magnitude of the temperature for the three scales represented was nearly equal when compared pass by pass. The magnitude of the mixing ratio values for the cell and cloud scales, however, was generally more than twice that recorded for the bubble scale.

4.5 Cloud Environment

Some of the effects of the cloud system upon its immediate environment are indicated in the previous illustrations and discussions. These effects are discussed below. In addition, portions of the monitoring pattern covered areas 10 to 15 n mi ahead and behind of the westward moving system. Analyses of these data are presented and discussed in this section.

Figure 14 shows the structure east (solid line) and west (dashed line) of the seeded area for the 550 mb level. The temperature and moisture profiles again exhibit the strong gradients associated with the northern edge of the ITCZ convection. A temperature difference of about 2C and a mixing ratio difference of about 4 gm/kg over a distance of 4 n mi occurred.

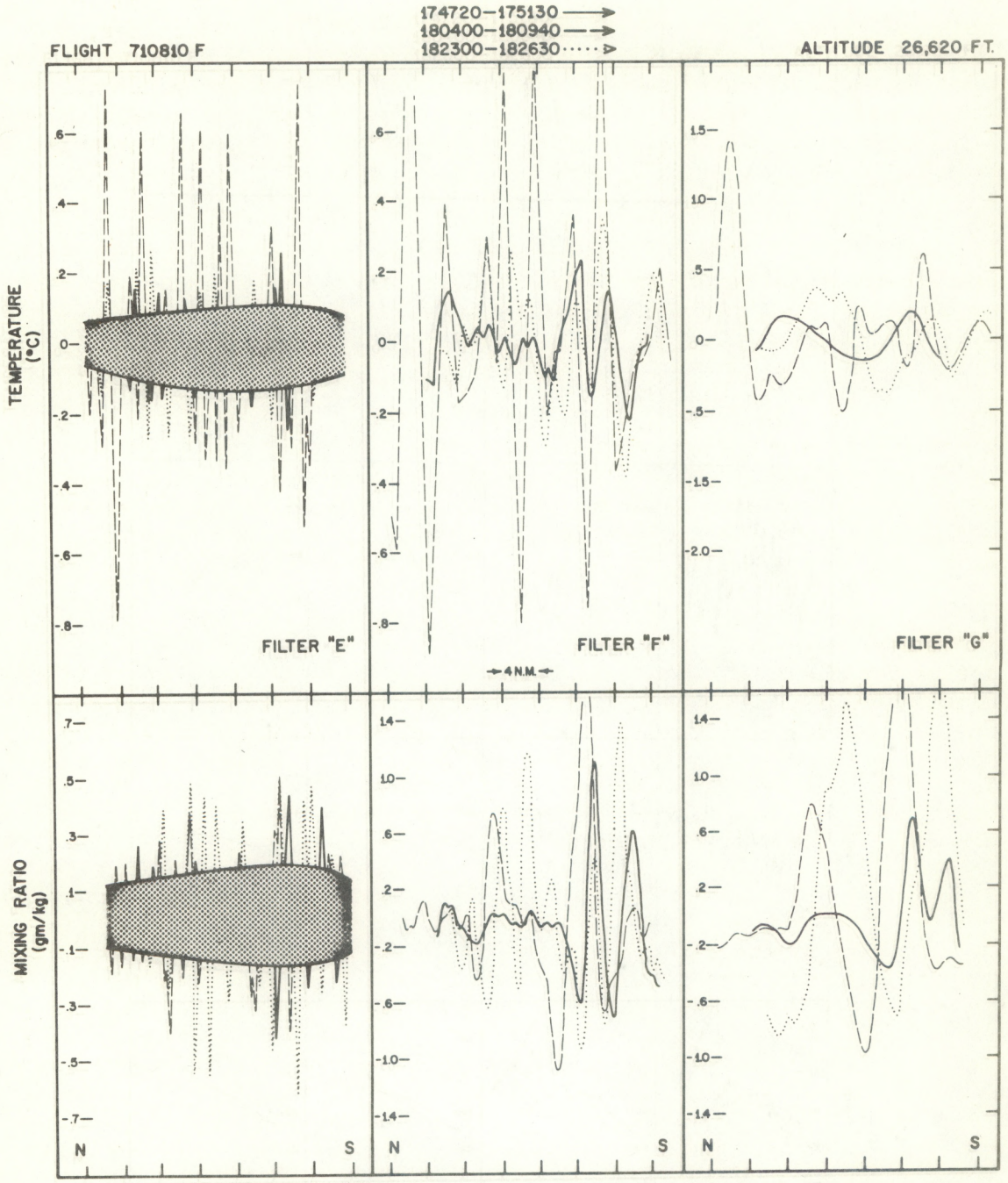

Figure 13. Band filtered temperature and mixing ratio profiles for north-south passes through the seeded cloud area at the 350 mb level. (Filters same as for fig. 11.)

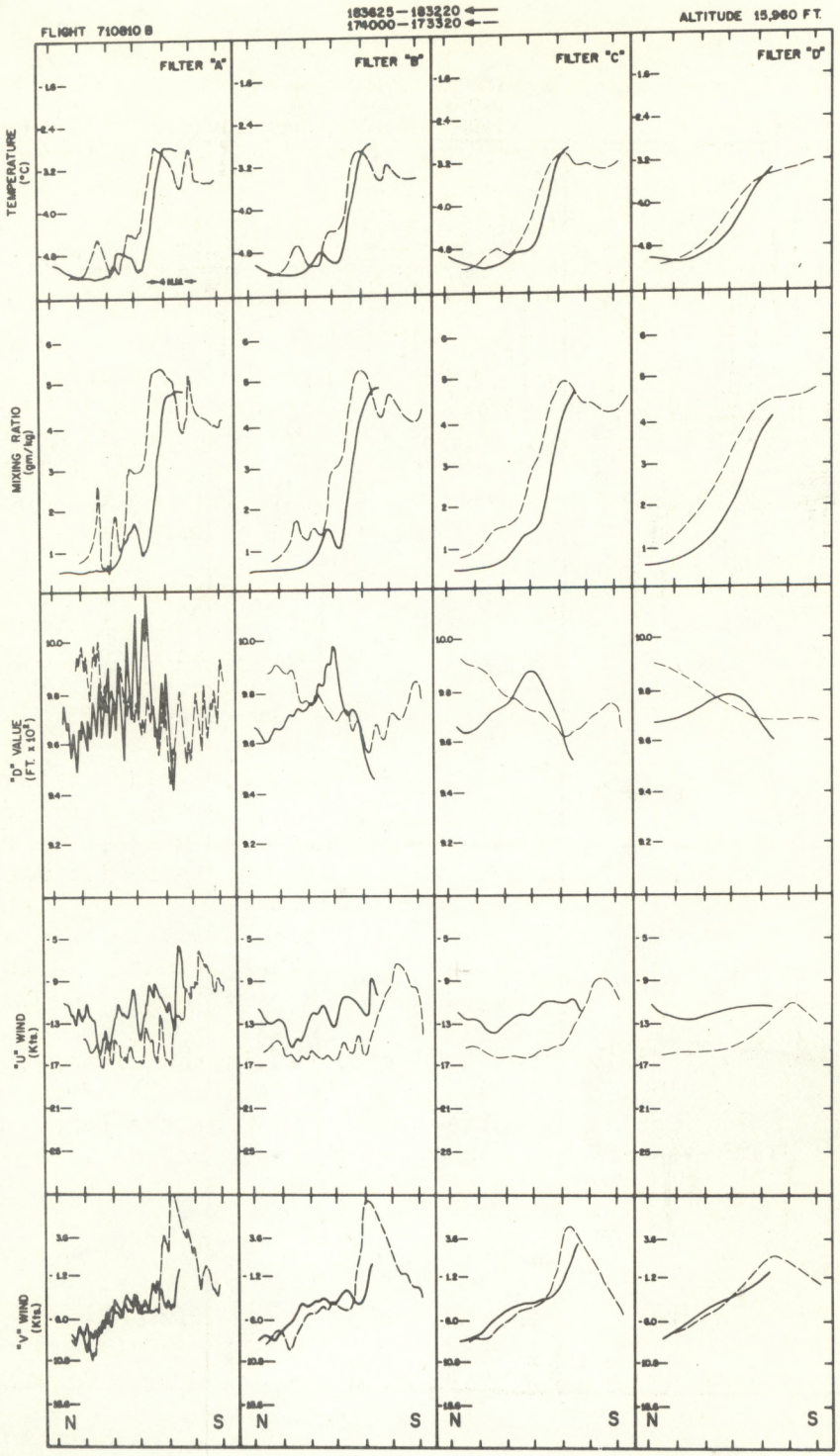

Figure 14. Filtered temperature, mixing ratio, "D" value, and u and v component profiles for north-south passes east (solid line) and west (dashed line) of the seeded cloud at the 550 mb level. (Filters same as for fig. 10.)

The maximum temperatures on these passes were 1C to 2C colder than those recorded on the cloud passes. The recorded mixing ratios indicated very dry conditions on the northern edge of the system and values approaching saturation on the southern end of the passes. Probably the most significant feature of these two sets of profiles is that they are nearly identical in the temperature and moisture fields, especially for the longer wavelength features (fig. 14 "C" and "D").

The "D" value and wind speed fluctuations were considerably less for these passes than for the passes through the cloud congested area. These fluctuations were generally less than 1 mb. The wind components indicated some possible convergence (u component) at this level where the wind speed on the west side of the system was less than that recorded on the east side. However, well-developed clouds were near these flight legs and probably had localized effects on these measurements.

The band filtered quantities for the above passes (not illustrated) indicated reductions of one-third to one-half in the amplitudes of the response obtained when compared with similar presentations for the seeded cloud area. Small scale features show that the area west of the system seemed to be slightly more disturbed than that to the east.

Figure 15 shows profiles of temperature, mixing ratio, and u and v wind components obtained at the 350 mb level east (solid and dotted lines) and west (dashed line) of the seeded cloud area. The temperature profiles indicated only small horizontal fluctuations with most of the variations contained in the small-scale features. Also, little difference was noted for the smooth profiles ("C" and "D") infront of and behind the system. This condition was similar to that noted over the seeded cloud area and, in fact, the mean temperature was nearly identical (-23C).

Significant differences were recorded in the mixing ratio for these passes (fig. 15). The smallest values were east of the westward moving system, but note that this was the first of the three passes. Earlier (fig. 12) it was shown that the moisture values increased with time over the seeded cloud area at this level. The clouds became larger and persisted through the monitoring period (figs. 4 and 5). Cloud development with increasing time was apparently the major contributor to the moisture distribution rather than the location of the pass. This assumption is further substantiated by both the latest and earliest passes being east of the system, and the moisture level nearly doubling during the 30 min period between the time of these passes.

The u and v wind components again showed large horizontal fluctuations. The larger scale structure ("D") showed some speed divergence in the u component, averaging near 9 kt east and 13 kt west of the seeded cloud. Some cyclonic rotation also appeared in the mean larger scale wind components. However, we must be cautious in interpreting these winds since all passes were near rather large clouds.

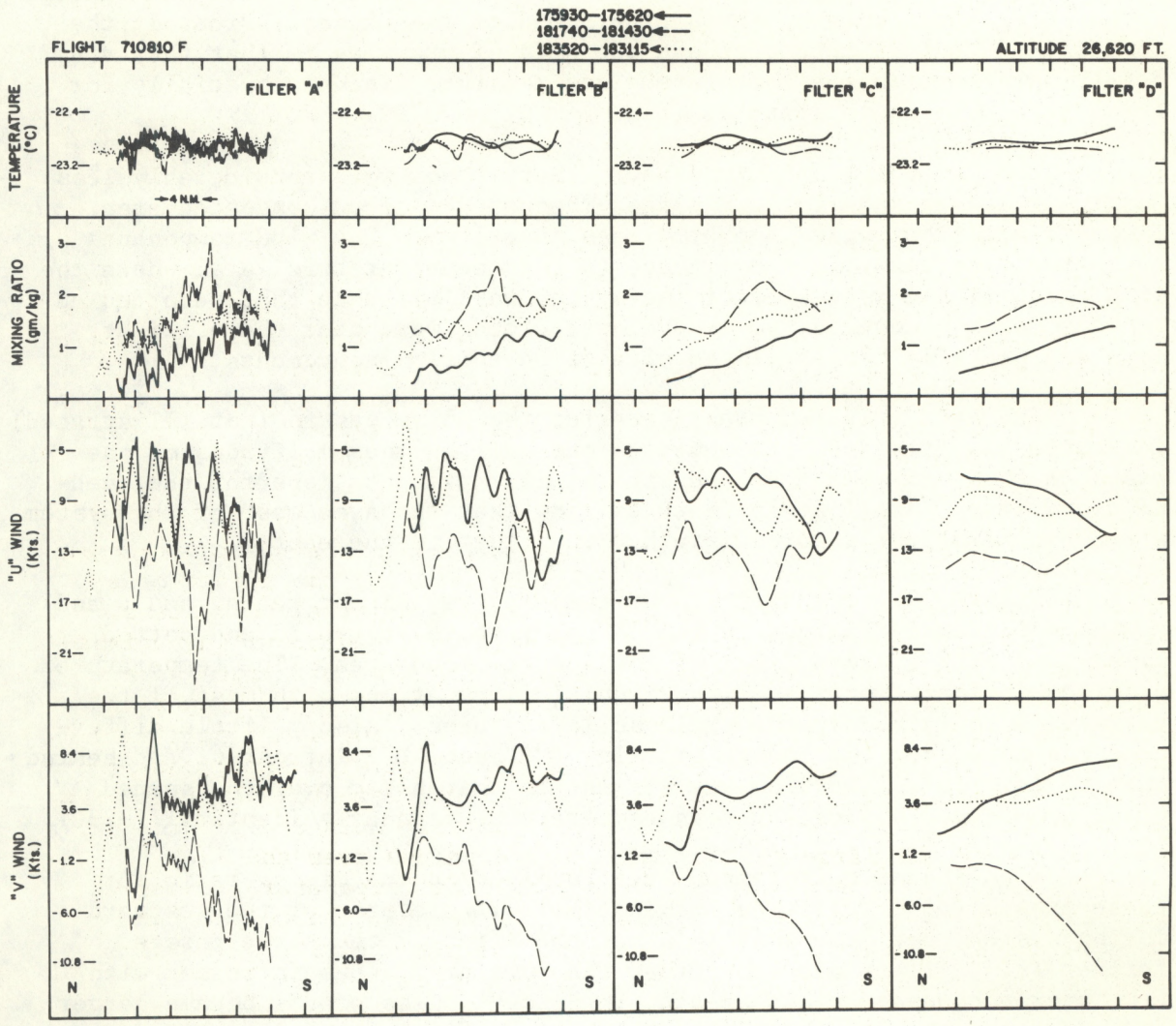

Figure 15. Filtered temperature, mixing ratio and u and v wind components profiles for north-south passes east (solid and dotted line) and west (dashed) of the seeded cloud at the 350 mb level. (Filters same as for fig. 10.)

The bandpass filtered temperature and mixing ratio profiles for these passes (not illustrated) indicated the same magnitudes as those recorded over the seeded cloud area for filter "E". However, the response obtained by application of "F" and "G" was generally considerably less than for the corresponding quantities recorded over the seeded area.

We now summarize the apparent effects this convective system has upon its environment. Little difference was noted between the temperatures observed on either side of the seeded area at both the 550 and 350 mb levels. However, a temperature difference of about 1C to 2C was noted for these profiles as compared with those obtained in the seeded area at the 500 mb level. Almost no temperature difference was noted at the upper level between profiles obtained east, west, and over the seeded area. Moisture increase with time at the 350 mb level was the only change noted on either side of the seeding target. These semi-uniform conditions were probably due to the fact that the entire area was convectively active and that general mixing took place. Only localized variations were prominent, probably due to individual cloud circulations rather than the circulations on the cloud-group scale.

The most prominent feature present in the profiles of temperature and moisture presented earlier for the 550 mb level in the seeded area (fig. 10) was the cold dry region between the two major cloud systems. The vertical motion was small in this region, thereby discounting adiabatic expansion processes as a means of maintaining the cold area. The single most important contributor seems to be evaporative cooling from detrainment of particles from nearby clouds. This process is partially indicated by the area becoming warmer and more moist with time; thus, indicating greater mixing with the developing cloud elements. In fact, the last pass through the area indicated rather uniform moisture conditions, especially over the large-scale. The average values over the 20 to 30 n mi pass showed little net change in moisture or temperature. However, the strong moisture gradient and, to a lesser degree, the temperature gradient associated with the northern edge of this activity were maintained throughout the monitoring period at this level.

The profiles at the upper level (350 mb) indicated a gradual increase of moisture during the 1-hour monitoring period. The temperature remained relatively steady when averaged over the cloud area. These two factors resulted in a net increase of about 3C to 4C in the equivalent potential temperature. The total change then indicates an increase in the depth of the moist layer and the erosion of the middle-level dry and cold layer, which results in an environment more conducive to greater cloud development.

4.6 Cloud Seeding Characteristics

The Simpson-Wiggert cumulus cloud model (Simpson and Wiggert, 1969) was run using a sounding composited from aircraft data, the Barbados sounding at 1200Z August 10, 1971, and other upper air data collected downstream in the ITCZ. The results of the cloud model calculations indicated that the active rising cloud bubble had to be relatively large in order to develop. Clouds with bubble diameters of 2000 m reach heights of about 25,000 ft in this environment. If the rising bubble diameter was 3,000 m then unseeded cloud tops reached heights of near 30,000 ft. The additional growth due to seeding was only about 2,000 ft for the 2,000 m cloud updraft diameter while seeding of the 3,000 m case results in about 13,000 ft of additional growth (fig. 16).

The RHI radar composites (fig. 5) showed average cloud tops to be about 25,000 to 30,000 ft before seeding. The seeded cloud then grew to a height of at least 39,000 ft while surrounding clouds increased horizontally, but their cloud tops remained in the 25,000 ft to 30,000 ft range. These values indicate that the cloud model with cloud diameters of 2,000 to 3,000 m accurately represented the observed unseeded and seeded cloud growths. Also, if we take the widths of the sharp updrafts indicated in figure 6 as being representative of the size of the rising bubble, then these cloud diameters are quite reasonable. The predicted liquid water content in the form of precipitation size particles is about twice as large as that recorded, but only about one-half the adiabatic value at the 550 mb level. Predicted vertical velocities at this level ranged from 8 to 13 m/sec, depending upon which radius was used. These values are close to those recorded on the pass through the cloud just before seeding.

To summarize the seeding characteristics, we find that the seeded cloud grew much more than surrounding clouds. Admittedly, this cloud system was chosen for its potential seedability and on its own may have grown more than the surrounding clouds. However, the parameterized cloud model successfully predicted the growth potential of this cloud as well as the characteristics of the unseeded clouds. The training of the flight crews was successful in that they picked a proper seeding candidate and delivered the seeding agent to the proper area as evidenced by the fact that the cloud reached its predicted growth potential.

5. CLOUD GROUP II STRUCTURE (1850 to 1945)

The second cloud group was 40 to 50 n mi WNW of cloud group I. The system basically consisted of a disorganized east-west line of small clouds with tops averaging near 15,000 ft.

The system was on the extreme northern edge of the convective activity associated with the ITCZ. Personnel on the seeder aircraft

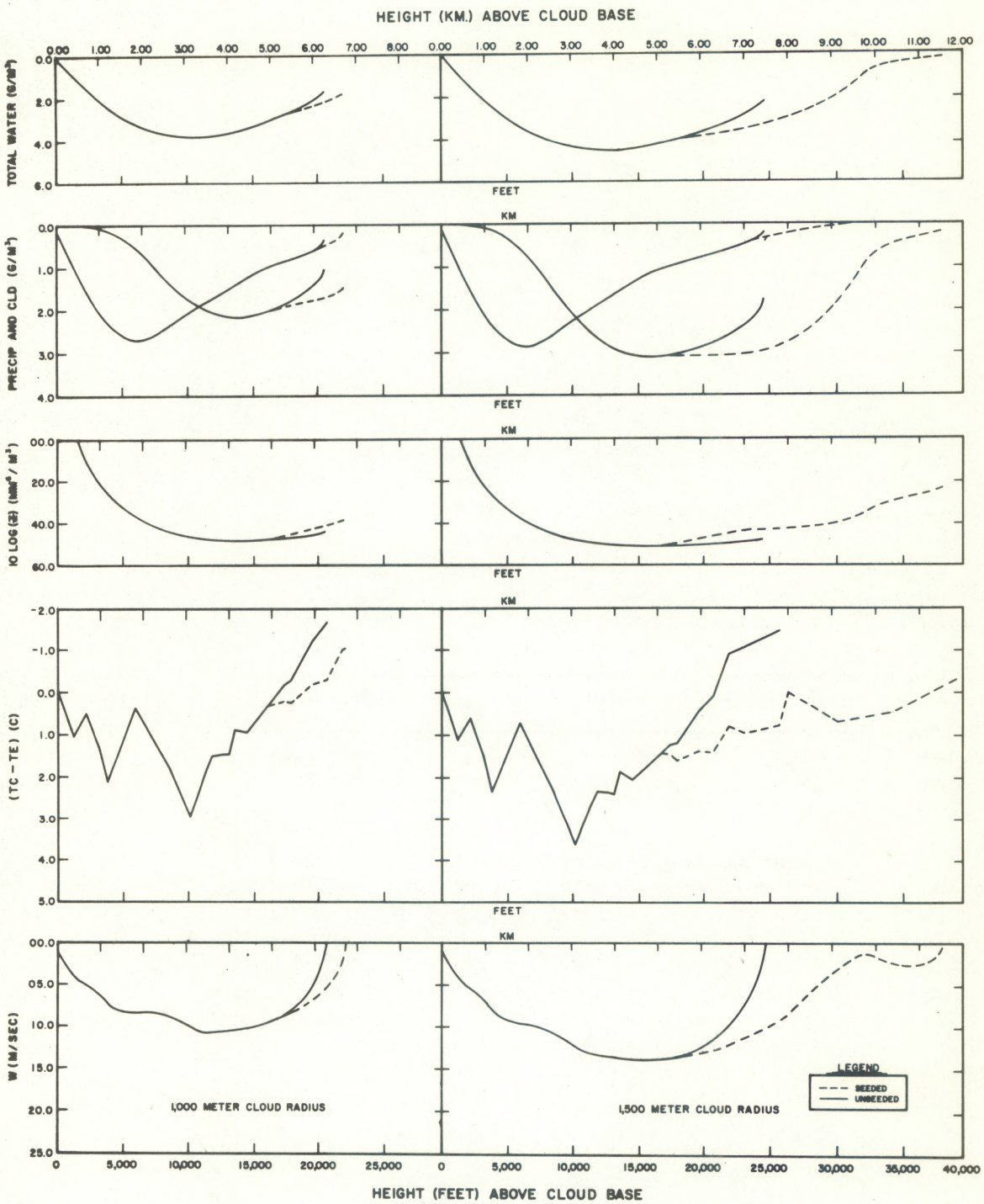

Figure 16. Model results for a sounding constructed for cloud group I using the Simpson-Wiggert parameterized cloud model with a cloud base of 950 mb. The solid lines are for the natural cloud and the dashed lines represent seeded cloud for the two cloud radii of 1,000 and 1,500 m.

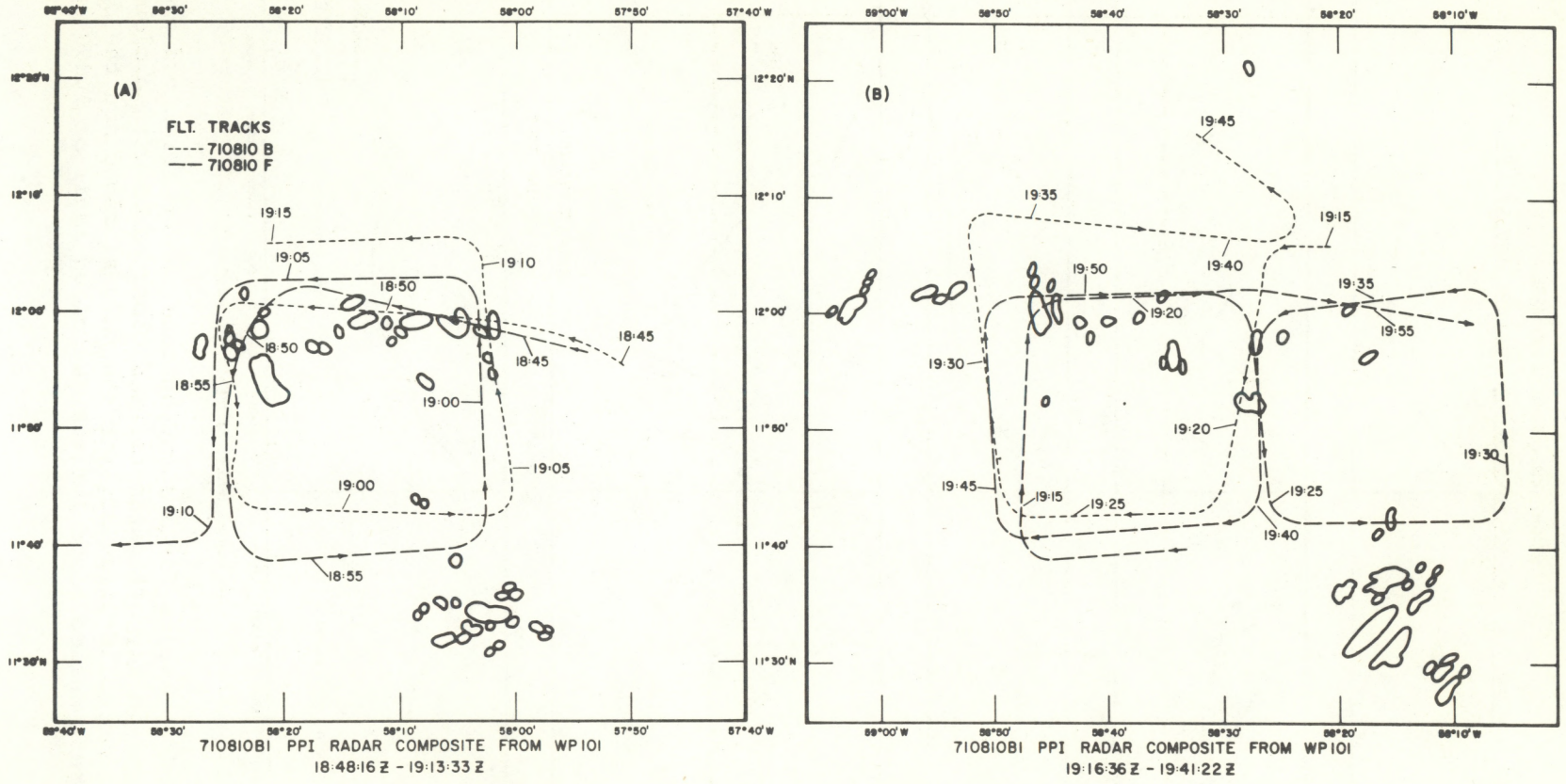

Figure 17. PPI radar composites for cloud group II and superimposed aircraft tracks.

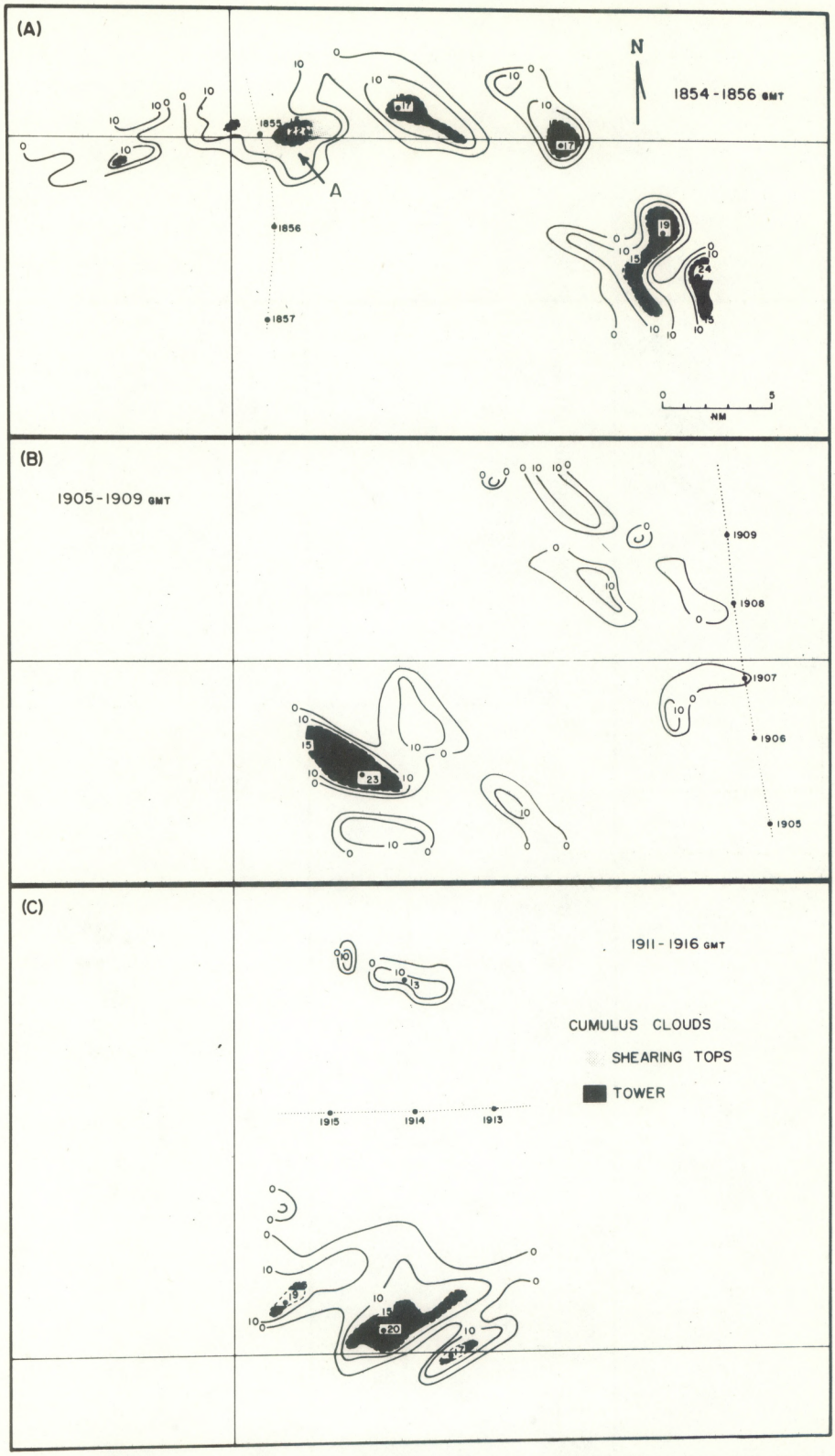

Figure 18. RHI radar composites for cloud group II and superimposed aircraft track.

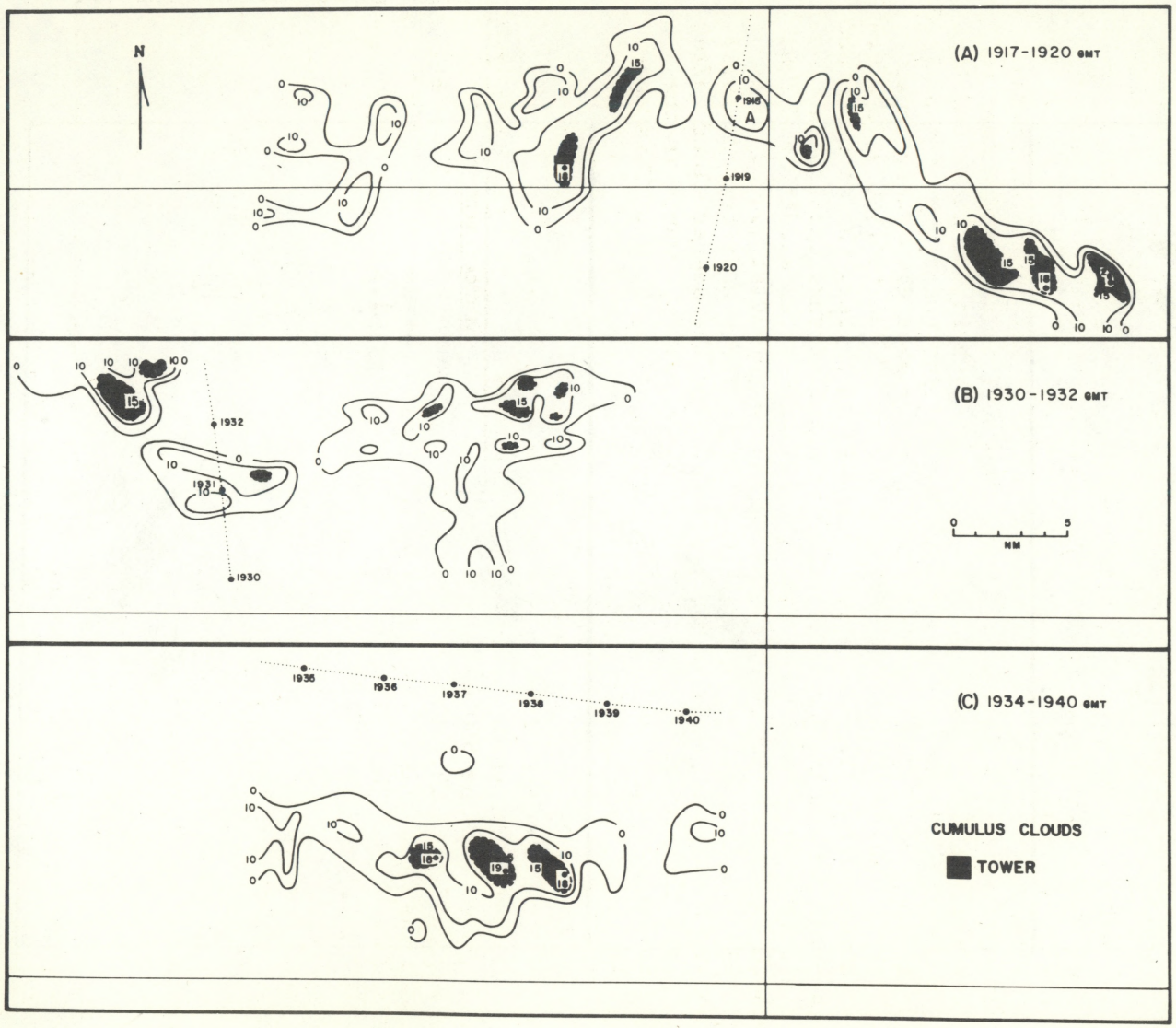

Figure 19. RHI radar composites for cloud group II and superimposed aircraft track.

selected a cloud at 1850Z and dropped two pyrotechnics into its 20,000 ft cloud top. At 1924Z a second cloud or turret in this cloud group was seeded with one pyrotechnic when the top was near 18,000 ft.

5.1 Radar

Figure 17 shows composites of the PPI radar structure of the cloud system. The presentation also includes the superimposed aircraft tracks and was obtained in the same manner as for figure 4. There was considerably less activity associated with this system than group I. Also, no major area wide development was observed during the monitoring period.

Figures 18 and 19 show a time sequence of RHI radar composites for this system. These composites were generated in the same manner as discussed earlier for figure 5. Only a slight shearing of the cloud tops occurred during the monitoring period. The maximum radar top of the cloud seeded at 1850Z was 22,000 ft five minutes after seeding. Other radar cloud tops in the immediate vicinity were about 17,000 to 19,000 ft above the sea surface (fig. 18A). Approximately 13 min later, the seeded cloud radar top was less than 20,000 ft (fig. 19A). Observers onboard the seeder aircraft noted that the cloud grew rapidly after seeding and then dissipated rapidly. Upon penetrating the seeded cloud at 19,000 ft at 1908Z, the seeder aircraft experienced no significant updraft. At 1915Z, an observer noted that the top had separated from the seeded cloud "after it had grown much taller." Radar tops of other cloud elements in the cloudline ranged from 15,000 to 20,000 ft (fig. 19 A, B, C). This condition persisted at least through the next 20 min.

5.2 Vertical Velocities

The vertical velocity profiles computed for the 550 mb level are shown in figure 20. Observers indicated that the flight through the cloud was bumpy just after seeding. Two distinct up- and downdrafts were recorded on this pass (dashed line) with maximum values exceeding 6 m/sec. Other smaller oscillations were noted in the nearly radar echo free area south of the seeded cloud. The maximum radar cloud top was about 22,000 ft at this time (fig. 18 A). The cloud top was separating from its base by the time of the next pass through the echo area. However, a maximum updraft of near 8 m/sec was recorded. Again, smaller vertical velocities of about 2 m/sec were recorded in the relatively radar echo free area south of the main cell.

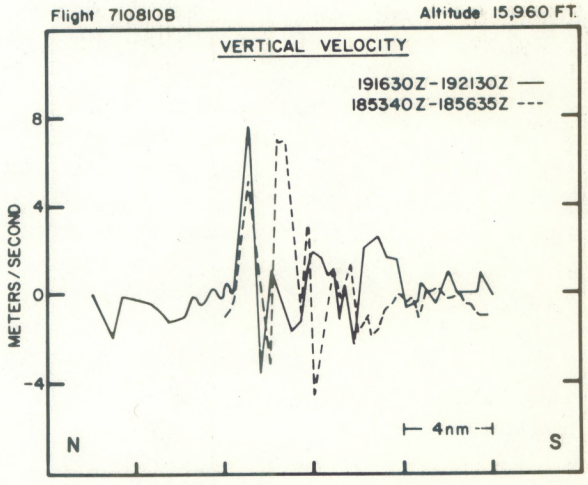

Figure 20. Vertical velocities recorded on north-south passes through the seeded cloud area at the 550 mb level.

5.3 Equivalent Potential Temperature

The equivalent potential temperature profile obtained on the first pass through the seeded cloud at the 550 mb level showed a broad zone of values between 335A and 340A (fig. 21). This area, of course, coincided with the convection and large vertical velocities discussed earlier. The gradient was near 20C over less than 4 n mi on the north end of the pass and decreased slowly on the south side of the system. By the time of the next pass some 20 min later, values ranged from about 322A to 330A where the 322A value reflected ambient conditions. The lowest values were recorded near the region where maximum values had been recorded on the previous pass. This condition reflects the dissipation phase of the cloud as discussed earlier and indicates that since the central and ambient values were nearly the same, entrainment of ambient air at this level had probably occurred. However, the values on the southern portion of the pass had increased over those recorded earlier.

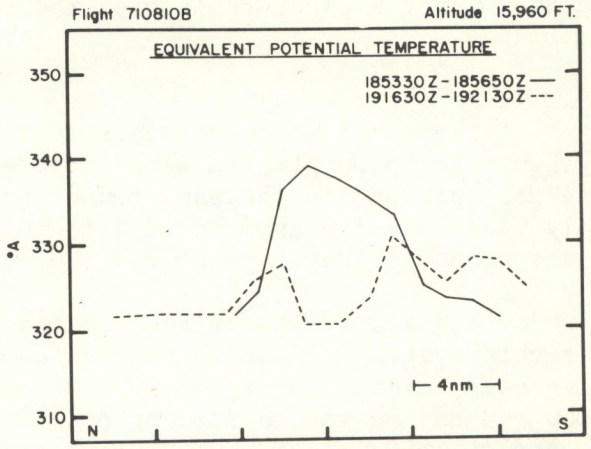

Figure 21. Equivalent potential temperature profiles recorded at the 350 mb level through cloud group II.

The equivalent potential temperatures recorded at the upper level (350 mb) essentially reflected stratified conditions (fig. 22). These measurements showed that few clouds had developed to this level during this period. However, it may be significant that a slight decrease over the entire level occurred during the later stages of the monitoring period.

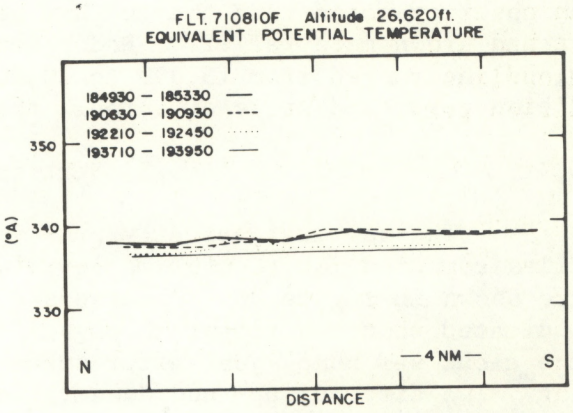

Figure 22. Equivalent potential temperature profiles recorded at the 350 mb level through cloud group II.

5.4 Temperature, Water Vapor, Pressure and Wind

The temperature profiles for (fig. 23) the 550 mb level were considerably different than the corresponding ones for cloud group I (fig. 10). However, the maximum value recorded on the first pass was

again located in the main cell, and a relatively cold area was located on the south side of the seeded cloud.

The maximum temperature recorded on this pass was about 1C colder than the corresponding value for cloud group I, but the minimum value to the south of the main cell was about the same for both cases. The temperatures recorded on the next pass indicated only a slight temperature peak in the remains of the main cell, but the strong temperature gradient and cold region on the south side of the cell remained. However, some slight warming occurred, and the temperatures recorded on the south end of the pass indicated a difference of about 1.5C. The mean temperature (filter "D") remained nearly the same except for this southern portion of the pass.

The mixing ratio profiles for these same passes (fig. 23) indicated nearly saturated values over the main cell during the first pass with extremely dry conditions prevailing north and south of the seeded cloud. By the time of the second pass, three peak values were recorded with a very dry region corresponding to the cold temperature discussed earlier. The peak values were less than saturation, but an increase in the moisture level was recorded on the southern end of the pass. However, extremely dry conditions continued to prevail on the north side of the remains of the seeded cloud. The larger scale feature (filter "D") indicated a net reduction of water vapor averaged over the pass.

The "D" value profiles (fig. 23) again showed relatively large horizontal fluctuations. However, the two most significant features are probably the net decrease in pressure (filters "C" and "D") of about 20 ft or 0.4 mb, and the cyclic nature shown best in filter "B" with a wavelength of about 3 n mi. This cyclic structure had been observed occasionally in previous "D" value profiles but had not been as obvious as this.

The wind components continued to reflect the ENE flow with large fluctuations in the cloud area (fig. 23). The average u component across the area (filter "D") remained near -15 to -17 kt while the v component was about -8 kt.

The band filtered temperature profiles for the 550 mb level (fig. 24) generally showed less amplitude than for corresponding profiles illustrated for cloud group I (fig. 11). This condition is especially true for the cloud scale motion (filter "G"). However, the relative amplitudes remained nearly the same. That is, the contribution from the smaller scale motions (filter "E") was about one-half that of the intermediate (filter "F") and one-third that of the cloud scale motions (filter "G"). The mixing ratio profiles indicated nearly the same magnitude of fluctuations as of cloud group I.

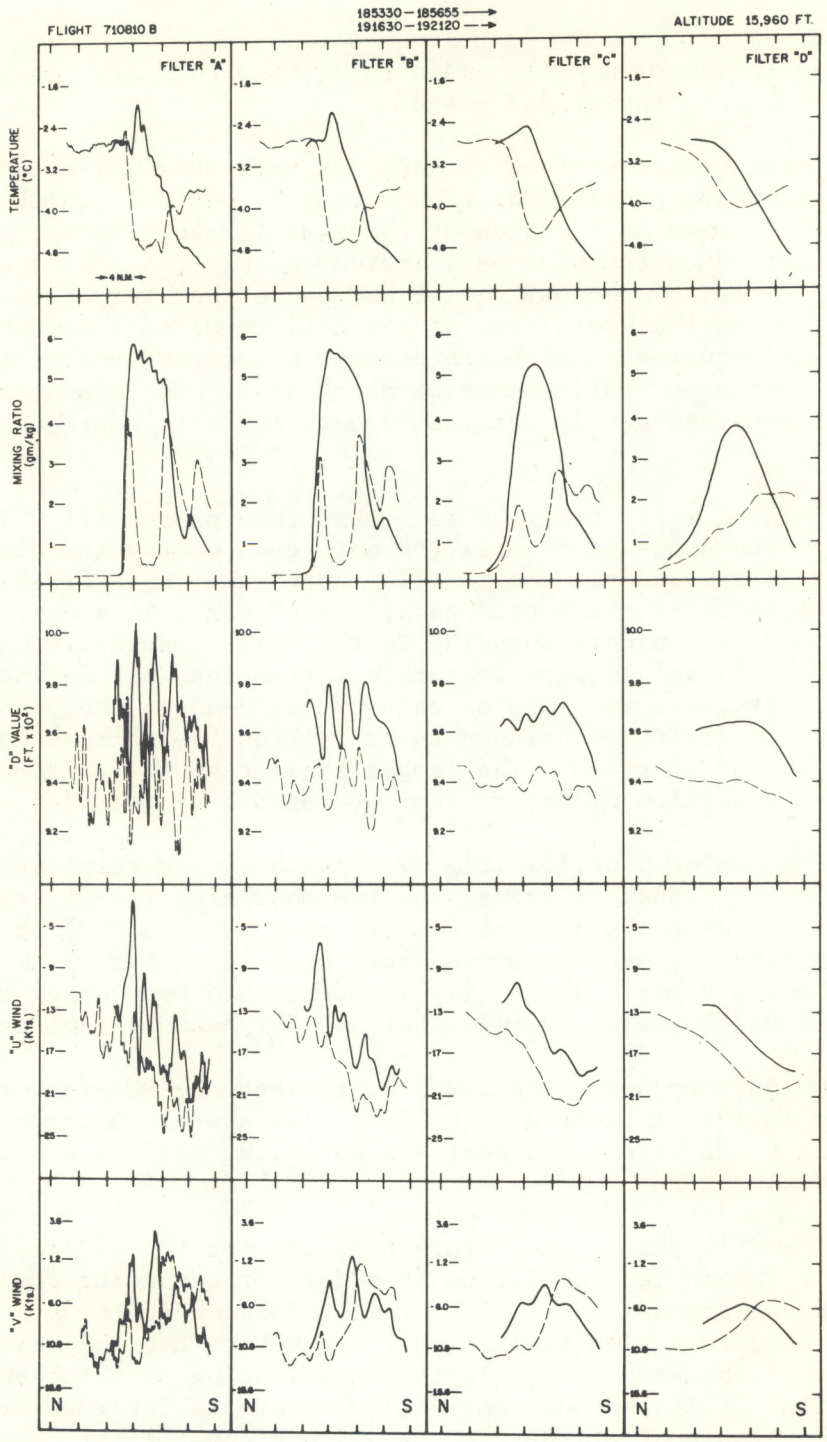

Figure 23. Filtered temperature, mixing ratio, "D" value, and u and v component profiles for north-south passes through the seeded cloud area at the 550 mb level. (Filters same as for fig. 10.)

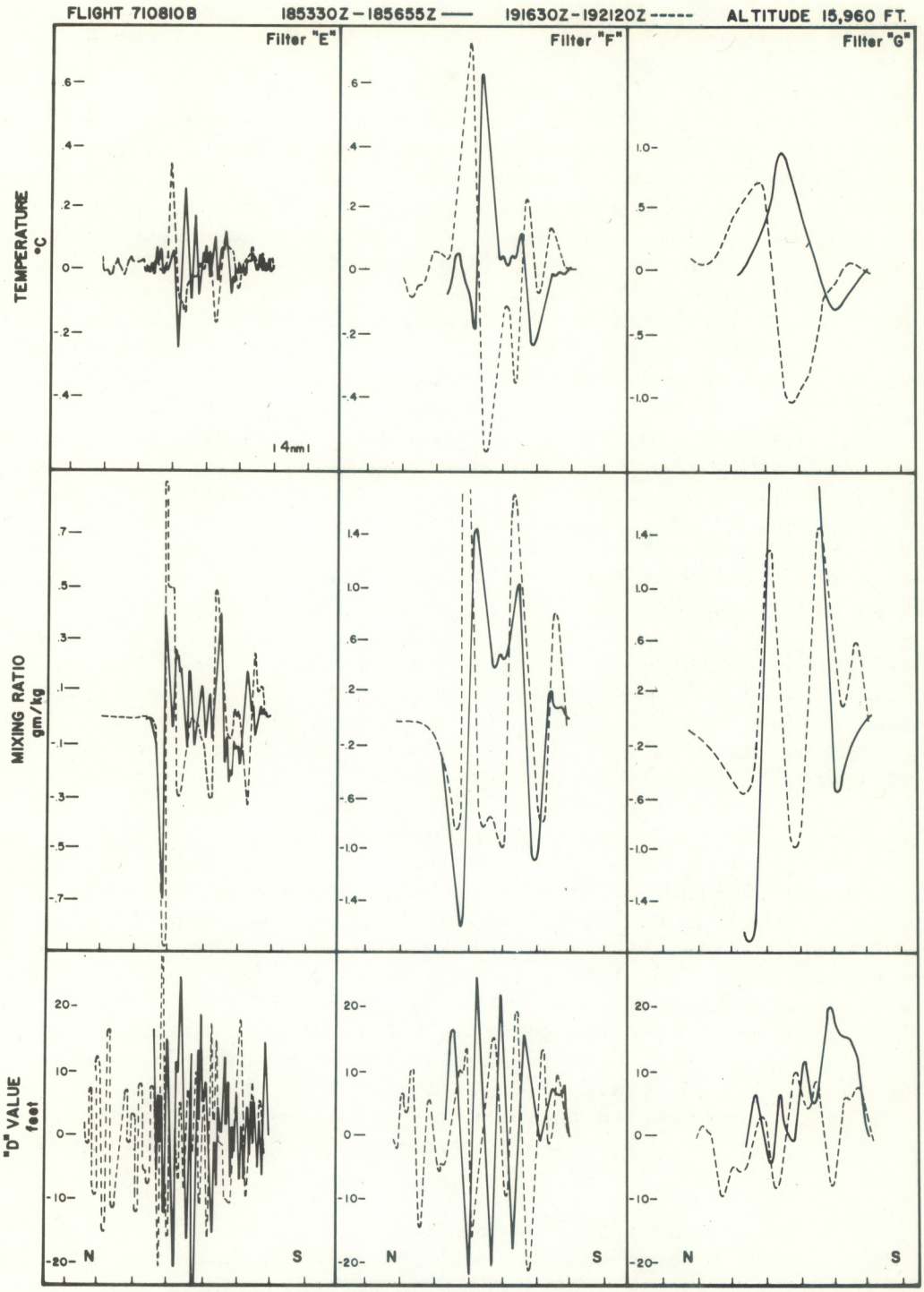

Figure 24. Band filtered temperature, mixing ratio, and "D" value profiles for north-south passes through the seeded cloud area at the 550 mb level. (Filters same as for fig. 11.)

The amplitude of the "D" value profiles was about one-third less for this case than for group I. Also, the cyclic nature discussed earlier is shown (filter "F") in figure 24.

The temperature, mixing ratio, and u wind component profiles for north-south passes through the seeded cloud area at the upper level are shown in figure 25. The temperature profiles showed only small horizontal variations. The northern end of the profiles indicated temperatures were about 0.5C colder than the middle or southern end. Also, the last profile indicated slightly colder temperatures over the area (0.3C) than were recorded on the three previous passes. The mean temperature for this level and area was about 0.5C colder than for the area over cloud group I.

The mixing ratio values indicated nearly undisturbed conditions but did gradually decrease with time. However, conditions were quite dry throughout the monitoring period. The u and v wind components again showed large horizontal fluctuations. The mean wind (filter "D") again was ENE at this level, but the speed was considerably less than that observed in cloud I and at the lower level. This factor of course should result in southeast shear of clouds that reached this level.

The band filtered temperatures and mixing ratios recorded at the 350 mb level (fig. 26) were reduced considerably over similar values recorded in cloud group I (fig. 13). This condition was especially true for the mixing ratio values, which indicated only minor fluctuations for cell (filter "F") and cloud-scale (filter "G") motion.

5.5 Cloud Environment

Figure 27 shows profiles of data recorded east (solid line) and west (dashed line) of the seeded cloud at the 550 mb level. The recorded temperatures indicated little net difference when averaged over the length of the pass (filter "D"). However, the center of this pass was slightly warmer than either end of both passes. A 0.8C difference existed between the central value and the end point values for the pass east of the seeded cloud. The central region of these two passes corresponds to the axis of the cloudline. It is significant to note that the center of the pass west of the main convective activity was not as warm as that for the east pass; but the ends of the pass were warmer than their eastern counterparts.

The water vapor profiles exhibited similar extreme dry conditions ahead of and behind the seeded cloud. The only exception was the peak in the west profile that was recorded as the aircraft passed over the cloudline.

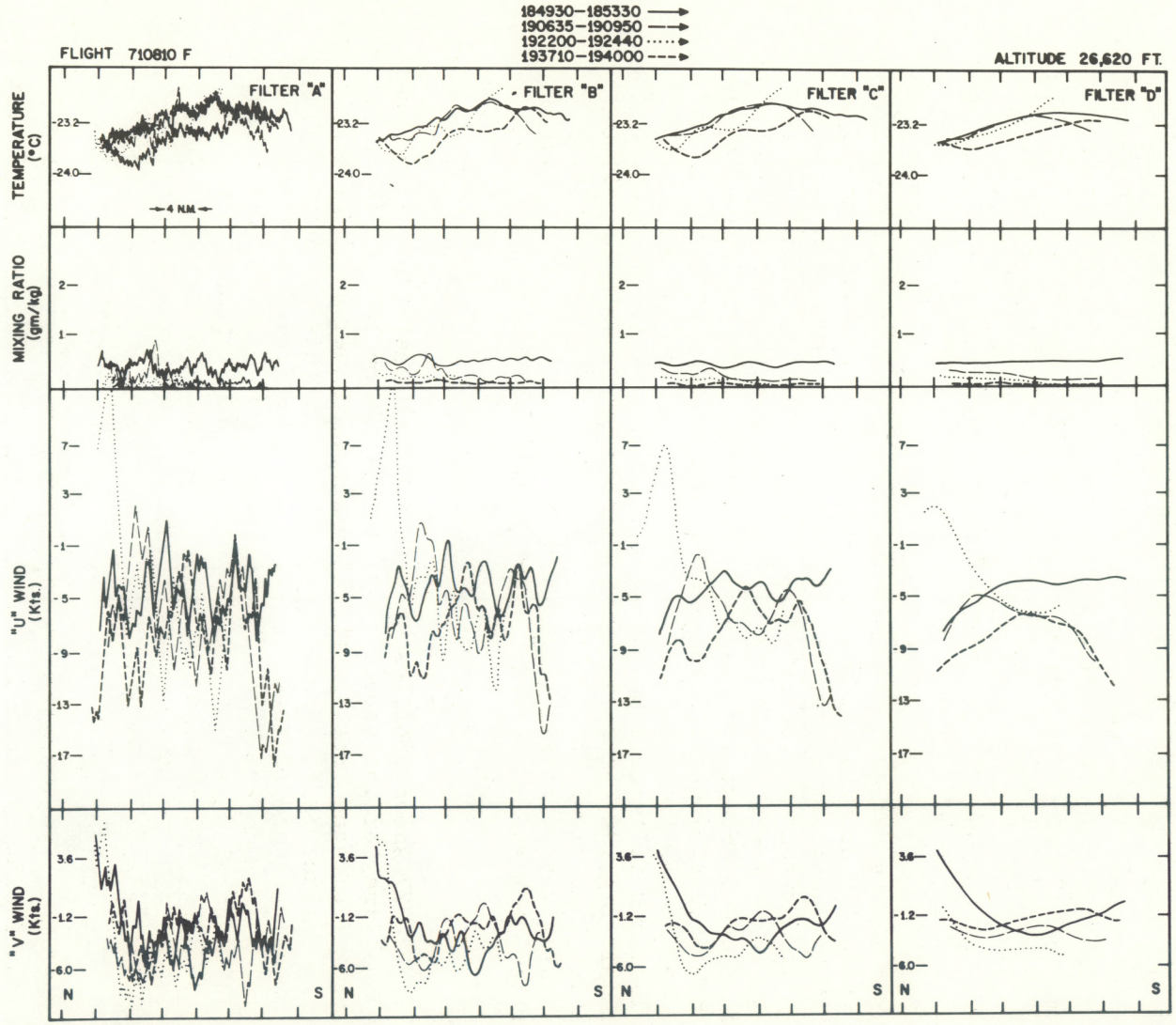

Figure 25. Filtered temperature, mixing ratio, and u and v wind component profiles for north-south passes through the seeded cloud area at the 350 mb level. (Filters same as for fig. 10.)

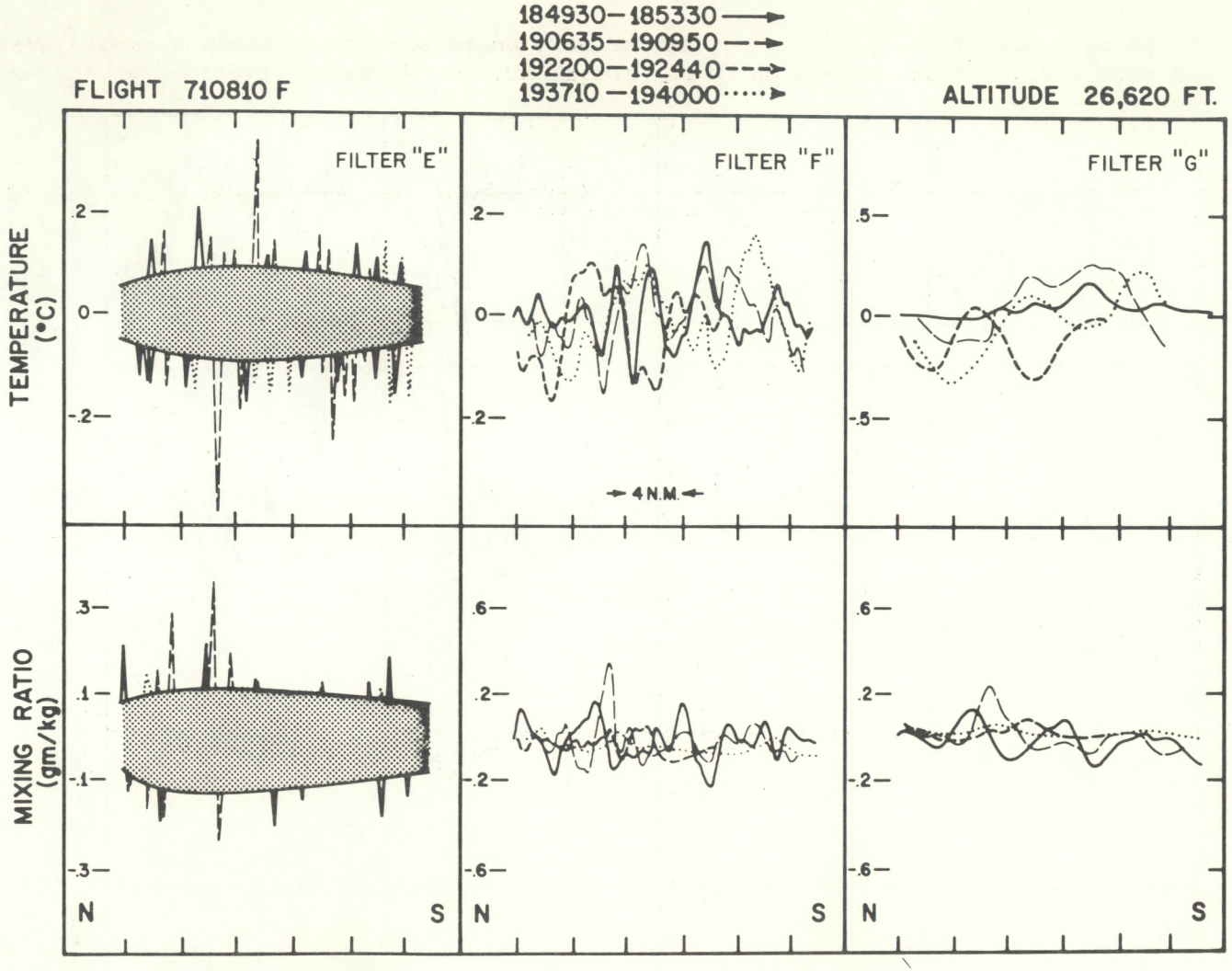

Figure 26. Band filtered temperature and mixing ratio profiles for north-south passes through the seeded cloud area at the 350 mb level. (Filters same as for fig. 11.)

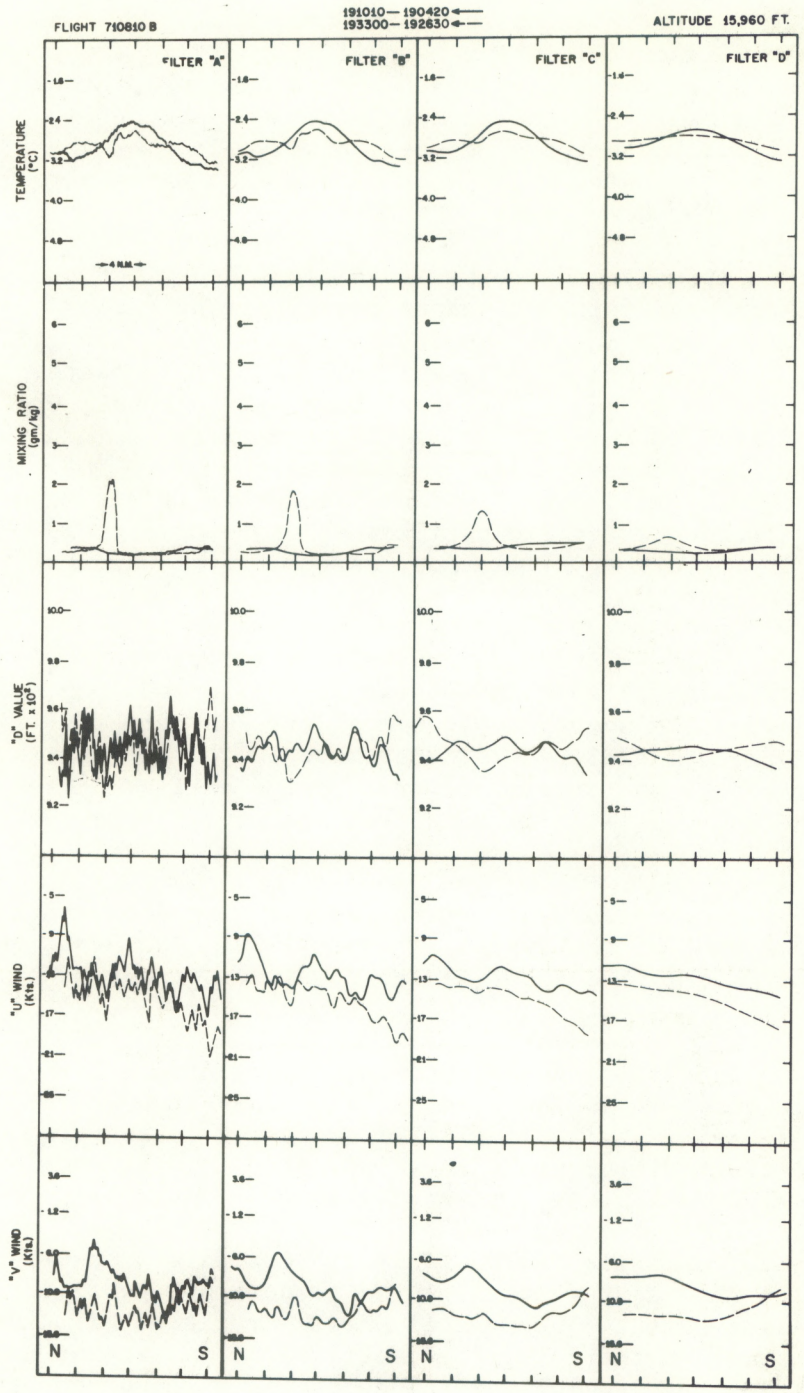

Figure 27. Filtered temperature, mixing ratio, "D" value, and u and v wind component profiles for north-south passes east (solid line) and west (dashed line) of the seeded cloud at the 550 mb level. (Filters same as for fig. 10.)

The pressure profiles indicated only small horizontal fluctuations and were nearly identical in the mean (filter "D"). The average value was nearly identical to that recorded on the second pass through the seeded cloud area (fig. 23). The horizontal wind components (fig. 27) were relatively steady but indicated some speed divergence over the area at this level. That is, the wind speed west of the area was generally 2 to 4 kt greater than on the east side.

The relatively undisturbed conditions described above were further verified in the band filtered temperatures, mixing ratios, and "D" values (not illustrated) for the 550 mb level. The small-scale (filter "E") temperature fluctuations were less than 0.1C, intermediate scale fluctuations less than 0.2C and the central warm area of about 0.5C was reflected in the filter "G" profile. The only prominent feature in the moisture profiles was the peak west of the seeded cloud. The "D" value profiles exhibited a cyclic oscillation of about 15 ft with a wavelength of 6 n mi and a secondary cyclic oscillation of about 5 to 10 ft with a wavelength of 3 n mi. A similar but larger 3 n mi wavelength oscillation was shown in figure 24.

The profiles of temperature, mixing ratio, and u and v wind components recorded at the 350 mb level east (solid and long dashed lines) and west (dotted and short dashed lines) are shown in figure 28. The maximum temperature differences were about 1C for all four passes. The largest horizontal variations occurred on the earlier passes, but by the time of the last pass some 50 min after seeding, the temperature profiles were quite smooth.

The mixing ratio profiles showed the greatest amount of water vapor located east of the system at about 1900Z. However, this same area was quite dry, nearly identical to the conditions recorded on the west side of the system 30 min later.

The u and v wind components again showed relatively large horizontal fluctuations even in these relatively cloud free areas. The mean u component was quite similar for all four passes. The v component, however, showed a distinct difference with values of 6 to 8 kt and 1 kt recorded on the east and west passes, respectively.

We now summarize the possible affects this system has upon its environment. The major feature in the temperature profiles for the east and west passes at the 550 mb level was the relative warm area over the cloudline axis. Furthermore, the central area was warmer and the north and south areas were cooler for the east pass as compared with the west pass. This thermal structure was probably a result of the release of latent heat east of the seeded cloud, which had been convectively more active than the western end of the system. Also, the stronger convective activity and the extreme ambient dry conditions apparently contributed to cooling the area on either side of the cloudline due to evaporation

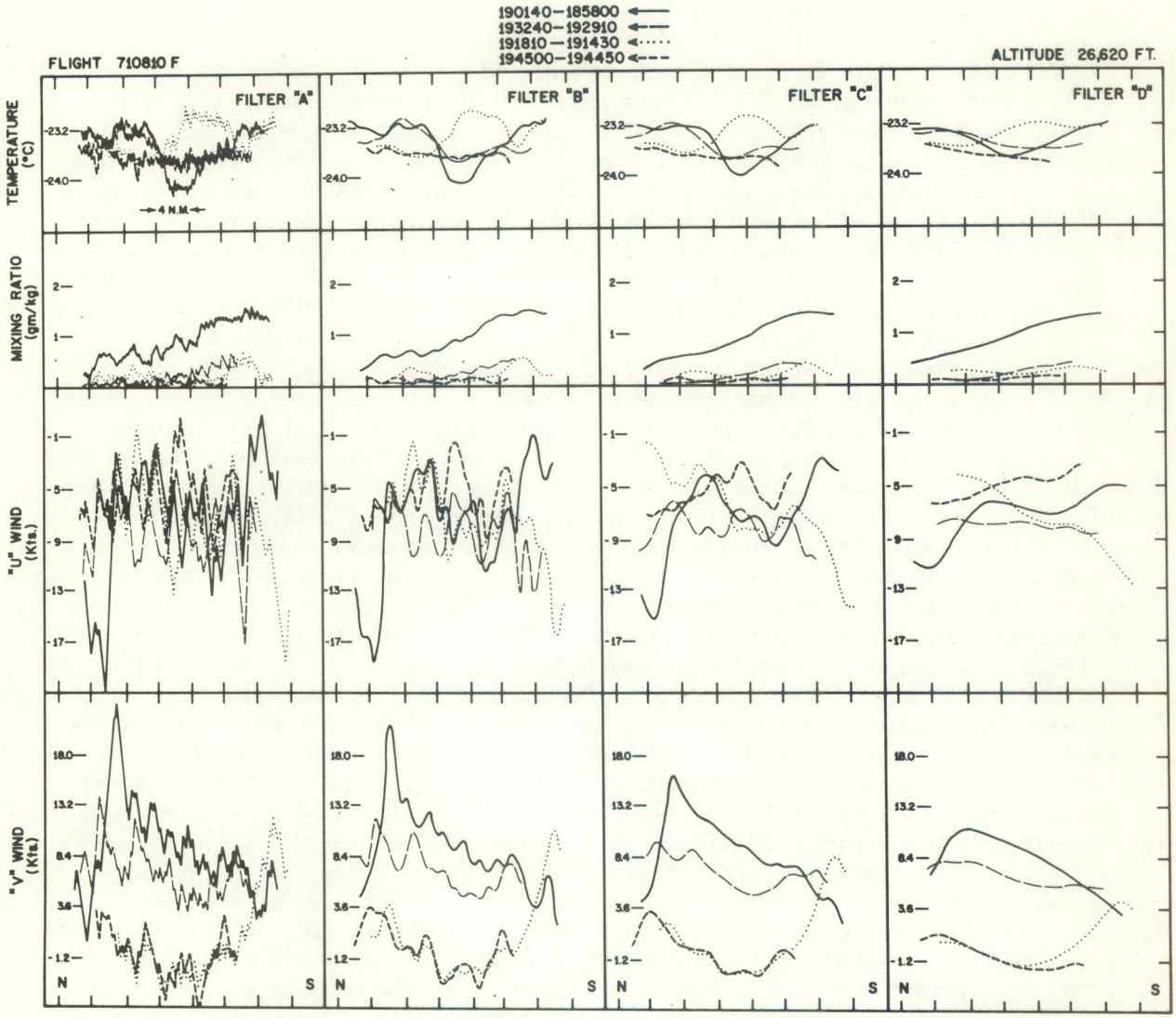

Figure 28. Filtered temprature, mixing ratio, and u and v wind component profiles for north-south passes located east (solid and long dashed lines) and west (dotted and short dashed lines) of the seeded cloud at the 350 mb level. (Filters same as for fig. 10.)

of cloud particles. The area was so dry that the convective activity had little net effect on the water vapor content at the 550 mb level in the larger scale (filter "D").

At the 350 mb level, temperature differences seemed to be largest on the early passes both east and west of the seeded cloud (fig. 28) when the convective activity seemed to be strongest (figs. 18 and 19). The temperature profiles became much smoother on later passes with some possible small net cooling occurring. The moisture values were largest on the first pass east of the system, but the convection appeared to have little net effect on the moisture content, as indicated on a pass some 30 min later after the convective activity in the area had decreased (fig. 17) and mixing with the extremely dry air had occurred.

The major feature present in the temperature and moisture profiles for the central region at the 550 mb level was the decrease in the cloud size, as reflected by the mixing ratio profiles, and the maintenance of the cold region on the south side of the seeded cloud. A process of evaporated cooling, similar to that hypothesized for a similar feature in cloud group I, probably maintained the cold region. The second pass indicated a trend toward increasing water vapor content and warmer temperatures at this level. Visual observations indicated that the cloud had grown rapidly after seeding. The cloud top then sheared or separated from its base the break being in the extremely dry region near the 500 mb level - and began to dissipate rapidly. This process of the rapidly developing cloud top shearing off and separating is shown in figure 29 and schematically in figure 30. The sequence of events is from east to west (A-C). The mean wind components indicate that the remains of the cloud top drifted south and east of its base (fig. 29). This overhanging or separating cloud probably supplied the particles for evaporative cooling on the south side of the cloud. The water vapor in this area was about twice that of ambient values but still was quite dry. At about 1920Z, the peak in the mixing ratio profile 6 n mi south of the base of the seeded cloud probably coincided with the remains of the dissipating cloud top. No moisture peak was noted on the previous pass through this area. Also, no echo was displayed by the 3 cm RDR radar, which would imply that any particles present were quite small. The structure at the 350 mb level indicated an area wide decrease of water vapor content with time and a possible slight cooling. This condition may just reflect the general decrease in the amount of convective activity that reached that level. The vertical velocities recorded between clouds indicated nearly neutral conditions except at the edges of the clouds.

5.6 Cloud Seeding Characteristics

A sounding was constructed for the second cloud area using the aircraft data and other data similar to those used for cloud group I. The major difference between the two soundings was that the environment of the second cloud area was considerably drier at the upper levels than

Figure 29. Seeded cloud with shearing top at 185810Z.

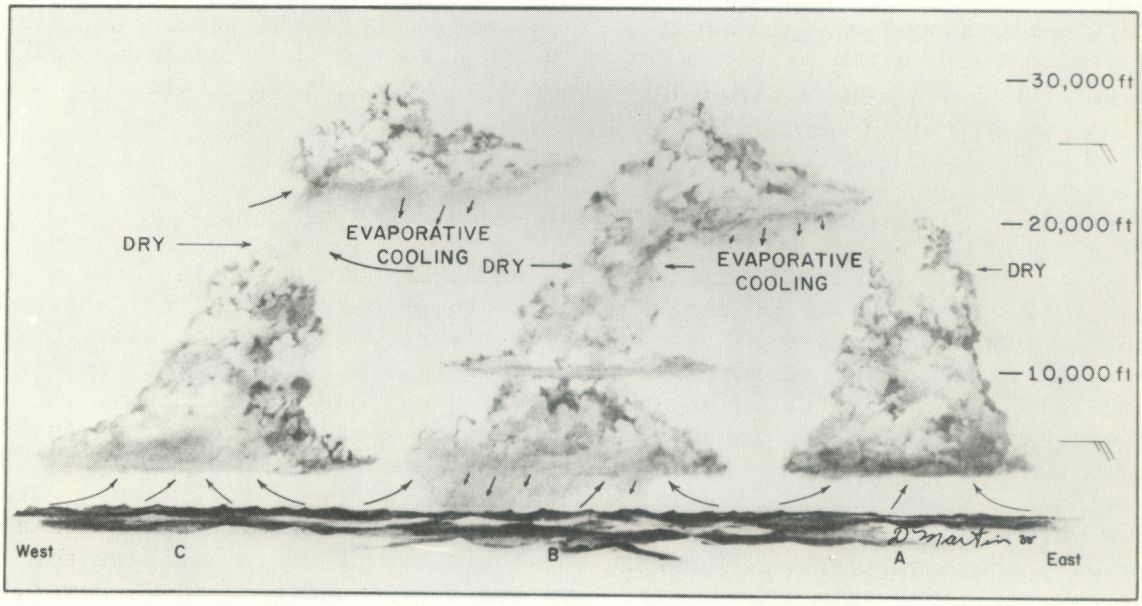

Figure 30. Schematic model of a cloud undergoing rapid growth and separation in a middle level dry layer and light shear.

the first. Also, another relatively dry layer was observed near the 700 mb level. The Simpson-Wiggert parameterized cloud model was run using the constructed sounding. The results of these computations (fig. 31) indicate that a cloud had to be quite large to have seeding potential in this environment. The model cloud with a rising plume diameter of 2,000 m reached a cloud top height of about 22,000 ft and additional growth of only 800 ft was obtained by seeding. If the rising plume was 3,000 m in diameter, then the unseeded model cloud tops reached heights of 28,000 ft and an additional 3,800 ft of growth could be obtained by seeding.

The RHI radar composites (figs. 18 and 19) showed average radar cloud tops of 15,000 ft to 23,000 ft. The cloud top was near 22,000 ft when seeded and grew rapidly. By the time of the second pass through the cloud some 20 min after seeding, it had dissipated somewhat by a process illustrated in figure 30. Other clouds in the area maintained nearly constant cloud heights during the monitoring period. In general, the sizes of the clouds seemed to decrease toward the west. These cloud dimensions correspond fairly well with the model cloud with a diameter of 2,000 m. The major updrafts illustrated in figure 20 are also of this same size. The measured draft scale vertical velocities reached near 8 m/sec which is comparable to the model predictions of 10 m/sec. No liquid water content was measured in this cloud. The predicted values of precipitation were only slightly less than for cloud group I (fig. 16).

To summarize the seeding characteristics, we see that the seeded cloud grew more than surrounding clouds. However, the rapid growth at the upper levels as well as slight shear and a middle level dry layer apparently caused a rapid decay of the cloud. That is, surrounding clouds appeared to maintain nearly constant heights during the monitoring period, while the seeded cloud grew rapidly and then within a short time, dissipated to well below its preseeding level.

6. SUMMARY AND CONCLUSIONS

The STORMFURY Cloudline exercises as discussed earlier have a two-fold purpose. The primary purpose is to prepare STORMFURY forces for an actual hurricane modification experiment while the secondary purpose is to collect data for studying seeding characteristics of clouds and their affects on the surrounding environment and other clouds. These exercises usually include using crews in a manner similar to that required for participation in an actual hurricane seeding operation. The period for these experiments is usually restricted to 7 to 10 days. Studies were made using satellite photographs to determine, with in certain bounds, the best time and location for these exercises to maximize the probability of getting the desired systems for investigation. However, the chances of having the ideal multiple cloudline situation occur in the operational area during this short time period remains small. Therefore, we cannot afford the luxury of random selection of seeding and

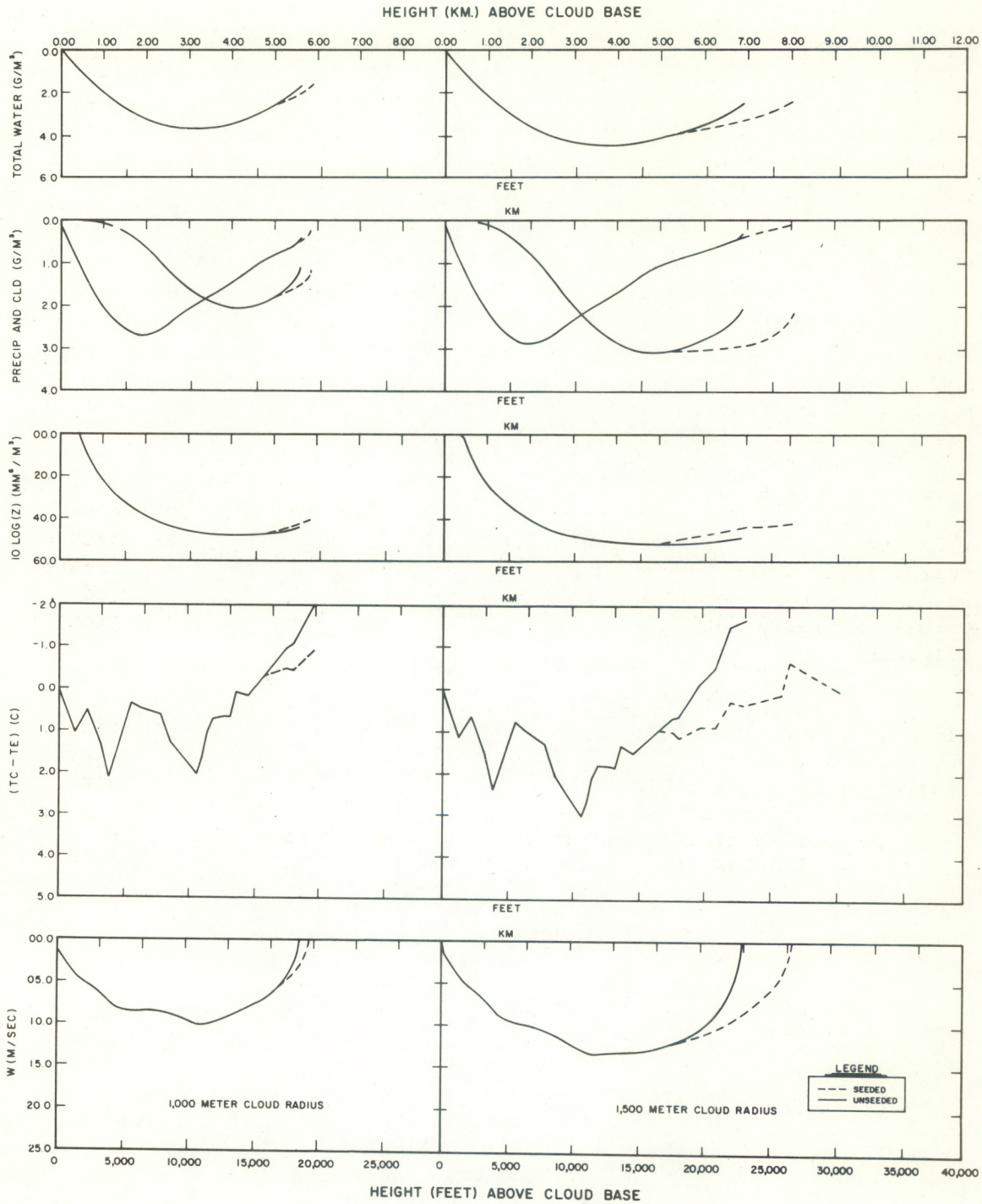

Figure 31. Model results for cloud group II using the Simpson-Wiggert parameterized cloud model with a cloud base of 950 mb. The solid lines are for the natural cloud and the dashed lines represent the seeded cloud for the two cloud radii of 1,000 and 1,5000 m.

control clouds but must seed clouds of opportunity to complete training portions of the program. The seeder aircraft crews therefore are trained to look for the best seeding prospects, but they will seed marginal clouds rather than cancel the mission because of the lack of the ideal situation.

These conditions preclude a thorough evaluation of seeding effects on clouds, since no unbiased control clouds are available. However, much can still be learned from these data about cloud dynamics and the affects of the clouds upon their environment. In both cases investigated, the seeded clouds grew more than surrounding clouds. This of course does not mean that this would not have occurred naturally, since the seeded clouds were selected for their apparent growth potential.

The first seeding was in an area of considerable convection that seemed to be on the increase, at least in areal coverage, throughout the monitoring period. The profiles obtained about 15 n mi east and west of the seeded area show the net change in temperature caused by the system seemed to be small at both the 550 mb and 350 mb levels. However, there seemed to be some localized warming and cooling near the convective activity at the 550 mb level. The profiles obtained some 30 to 40 n mi west of this system on the edges of cloud group II are probably more representative of the ambient conditions at the 550 mb level than those indicated in figure 14. When we compare these two sets of profiles we find that the average temperature was a little more than 1C colder at this level in the area of the massive convection than in the less disturbed area to the west. This apparent net cooling was probably a result of evaporation in the extreme dry layer, which occurred in all profiles at this level outside of actual convective elements. The duration of this condition is undetermined.

The temperature fields at the 350 mb level indicated no major difference between the ambient values of cloud group I and those of cloud group II (fig. 28). However, the effect of the convective activity in cloud group I was at least temporarily to increase the broadscale water vapor content at this level when compared with the ambient conditions.

The net effect of cloud group II on the cloudline scale environment seemed to be minimal. However, a condition that has often been observed is exemplified by this case, i.e. a rapidly developing cloud whose top becomes separated from its base and yet remains somewhat active for a few more minutes. This process is shown in figures 29 and 30. Note the clear area under the most active portion of the cloud top in figure 29. The main cloud base is northwest of the cloud top. This process was caused by wind shear with height and entrainment of very dry air from the layer near the 550 mb level. The result was that large localized gradients of moisture and temperature were created. The convective activity became more widespread, as for cloud group I, and these localized features eroded due to the mixing created by the increased activity. However, large gradients persisted for some time near the edges of these systems.

The total definition of these systems has not been accomplished. We would like to have similar measurements at lower levels to determine the vertical extent of these localized conditions, as well as larger scale measurements to determine mass flow characteristics. Also, we need to sample the air at various intervals in the wake of these systems to determine how long this condition persists and if it is long enough to significantly affect following systems. Hopefully, GATE or other future experiments will address these questions.

7. ACKNOWLEDGMENTS

The authors thank the NOAA RFF, U.S. Air Force and U.S. Navy aircrews as well as NHRL staff members who collected the data used in this study. In addition several past and present members of the NHRL staff participated in some phase of the data processing. These individuals include Mr. Clyde Dossett who performed the liquid water analyses, Mr. David Senn who digitized the RDR radar presentation, Mr. Bill Foltz who wrote the programs for plotting out the RDR composites, Dr. Toby Carlson who supplied his vertical velocity program and Mr. Richard Pasch who assisted in the early analyses of the aircraft data. Mr. Victor Wiggert of EML kindly supplied his program for the Simpson-Wiggert cloud model, which was used to compute seedabilities.

8. REFERENCES

Carlson, T. N. & R. C. Sheets (1971): Comparison of Draft Scale Vertical Velocities Computed from Gust Probe and Conventional Data Collected by a DC-6 Aircraft. NOAA Tech. Report ERL NHRL-91, 39 pp.

Hindman, Edward E. II (1970): "Cloud Particle Samples and Water Content from a 1969 Stormfury Cloudline Cumulus," Project STORMFURY Annual Report 1969, Appendix F, (National Hurricane Research Laboratory, Miami, Florida), pp F 1-6.

Sheets, Robert C. (1973): Analysis of STORMFURY Data using the Variational Optimization Approach, NOAA Tech. Report ERL 264-WMPO-1, 92 pp.

Simpson, J. and V. Wiggert (1969): Models of Precipitating Cumulus Towers, Monthly Weather Review, 97 (#7), pp 471-489.